Benzoate-Tolerant *Escherichia coli* Strains from Experimental Evolution Lose the Gad Regulon, Multi-Drug Efflux Pumps, and Hydrogenases

by

Jeremy P. Moore,[a]* Haofan Li,[a]* Morgan L. Engmann,[a] Katarina M. Bischof,[a] Karina S. Kunka,[a] Mary E. Harris,[a] Anna C. Tancredi,[a] Frederick S. Ditmars,[a] Preston J. Basting,[a] Nadja S. George,[b] Arvind A. Bhagwat,[b] Joan L. Slonczewski.[a#]

[a]Department of Biology, Kenyon College, Gambier, Ohio, USA.

[b]Environmental Microbiology and Food Safety Laboratory, Beltsville Agricultural Research Center, U.S. Department of Agriculture, Beltsville, MD, USA.

[#]Corresponding Author:

Joan L. Slonczewski, slonczewski@kenyon.edu

Department of Biology, Kenyon College, Gambier, Ohio, USA

*These two authors contributed equally to the work.

ABSTRACT

Benzoate, a partial uncoupler of the proton motive force (PMF), selects for sensitivity to chloramphenicol and tetracycline in *Escherichia coli* K-12. Genetic mechanisms of increased benzoate tolerance and decreased drug resistance were analyzed in strains isolated from experimental evolution with benzoate. Transcriptomes showed reversal of benzoate-dependent regulation, including the Gad regulon for acid resistance and multi-drug resistance (MDR). Benzoate-evolved strains knocked down the nitrate reductase *narHJ* and the acid-consuming hydrogenase Hyd-3, but upregulated OmpF and other porins that admit nutrients and antibiotics. Mutations were found affecting many genes of aromatic catabolism such as *folD* and *add*. Several candidate genes from benzoate-evolved strains had a role in benzoate tolerance. Growth with benzoate or salicylate was increased by deletion of the Gad activator *ariR*, or by deletion of the *slp-gadX* acid fitness island encoding Gad regulators and the MDR pump MdtEF. Benzoate growth was also increased by deletion of MDR component *emrA*, the RpoS post-transcriptional regulator *cspC*, or the adenosine deaminase *add*. Growth in chloramphenicol with benzoate was decreased by a point mutation in the RNA polymerase alpha-subunit *rpoA*, which appeared in one chloramphenicol-sensitive benzoate-evolved strain. Growth in chloramphenicol was also decreased by deletion of Mar activator *rob*, or of *rfaY* (lipopolysaccharide biosynthesis). Hydrogenase Hyd-3 deletion increased benzoate tolerance. Overall, long-term culture in the presence of benzoate or salicylate favors loss of MDR efflux pumps and of hydrogenases that generate a futile cycle of PMF; and favors upregulation of large-hole porins that increase uptake of fermentable nutrients and of antibiotics.

IMPORTANCE

Benzoate is a common food preservative, and salicylate is the active form of aspirin. In *E. coli*, benzoate derivatives upregulate multiple regulons that export antibiotics and other toxic products, and downregulate large outer-membrane porins that allow antibiotic influx. But benzoate or salicylate exposure causes energy stress by depleting the proton motive force. In the absence of antibiotics, long-term benzoate exposure selects against energy-spending systems such as multi-drug efflux pumps and the proton-consuming hydrogenase. Selection favors upregulation of porins that admit fermentable substrates but also allow entry of antibiotics. Thus, evolution with benzoate requires a tradeoff for antibiotic sensitivity. Benzoate and salicylate are naturally occurring plant signal molecules that may influence the evolution of microbiomes in plants and in animal digestive tracts. Effects on hydrogenase activity may be relevant to the biotechnology of hydrogen production.

INTRODUCTION

Escherichia coli and other enteric bacteria face high concentrations of organic acids, such as short-chain fatty acids that permeate bacterial cell membranes and acidify the cytoplasm (1, 2). Acids that permeate in the unprotonated form can lead to toxic anion accumulation (3, 4) and partly uncouple proton motive force (PMF) (5–8). Benzoic acid and salicylic acid (2-hydroxybenzoic acid, the active form of aspirin) are abundant in human diets in the form of food preservatives, pharmaceutical products, and natural plant secondary metabolites (9–12). Given the prevalence of benzoate derivatives in human diets, and in the plant rhizosphere (13), there are interesting questions as to their molecular effects on bacteria.

Benzoate and salicylate induce low-level resistance to antibiotics, via a large number of regulators including the Mar regulon (14) as well as poorly understood mar-independent pathways (15). The Mar regulon intersects with the Gad acid resistance regulon (16, 17) which includes a major region of acid-stress regulators and multidrug efflux pumps (MDR) (**Fig. 1**). Yet, experimental evolution with benzoate leads to loss of both acid resistance and resistance to the antibiotics tetracycline and chloramphenicol (18). Sequenced strains had lost MDR pumps and regulators such as *emrA*, *emrY*, and *marRAB.* Similarly, experimental evolution with a strong uncoupler, carbonyl cyanide m-chlorophenyl hydrazone (CCCP), yields strains that lose MDR pumps and regulators, with the exception of the EmrAB-TolC pump that exports CCCP (19, 20).

We hypothesize that as a partial uncoupler such as benzoate or salicylate depletes PMF, the cell incurs energy stress, which selects against MDR pumps that spend PMF. Constitutive induction of stress response pathways carries a heavy energetic penalty; thus, deletion or knockdown of constitutively expressed pathways confers an energetic advantage. The penalty could arise from the cost of protein production, which increases non-linearly with additional

transcription (21). In the case of acid stress, experimental evolution leads to loss of three acid-inducible amino-acid decarboxylase systems (22, 23). Alternatively, PMF expenditure has a fitness cost, as in the *lac* operon, where the major fitness cost of expression is the activity of LacY permease, driven by PMF (24).

Most of the benzoate-tolerant isolates from the evolution experiment (18) acquired a mutation affecting the *slp-gad* (Gad) acid fitness island (16, 25–27). The Gad island includes acid-resistance regulators *gadE*, *gadW*, *gadX* (28); periplasmic acid chaperones *hdeA* and *hdeB*; and the MDR efflux components *mdtE*, *mdtF* (29, 30) (**Fig. 1**). The major regulator GadE upregulates several acid-tolerance genes, including two glutamate decarboxylase isoforms (*gadA* and *gadB*), whose activity increases cytoplasmic pH by consuming protons via decarboxylation of glutamate (16, 27, 31, 32). The MdtEF-TolC complex exports antibiotics from the cytoplasm, driven by PMF. Our benzoate-evolved isolates (18) have acquired point mutations or deletions throughout *slp-gad*, as well as knock-out or point mutations in *emrA*, the membrane-fusion protein component of the EmrAB-TolC MDR pump (33, 34); *mdtA* (35, 36); and *emrY* (37). Other mutations affect MDR regulators such as *cpxA* (38), *ariR* (39), *arcA* (40), and *rob* (41).

In one population, benzoate has selected for deletion of *marRAB*, a multi-drug resistance operon which is induced by MarR binding salicylate or benzoate (15, 41). MarRAB has homologs throughout bacteria and archaea, and plays a role in many drug-resistant clinical isolates (42). In *E. coli*, salicylate or benzoate relieves repression of MarA, which regulates over 60 genes involved in antibiotic resistance such as AcrAB-TolC MDR pump (14, 43) as well as *hdeAB* within the *slp-gad* island (17). MarA downregulates the large porin OmpF, which admits nutrients and antibiotics (44). Many targets of MarA are also subject to MarA homolog Rob (41, 42), which had a mutation in one benzoate-evolved isolate (18). Additionally, one strain acquired

a mutation in the alpha subunit of RNA-polymerase which could affect the regulation of a wide array of genes. RNAP mutations have been shown previously to lead to unexpected phenotypes such as the downregulation of arginine decarboxylase caused by an *rpoC* mutation in an acid-evolved strain (45).

Here we report the resequencing of earlier populations from the benzoate evolution with fewer mutations to gain insight to the order in which mutations were acquired, and the existence of multiple populations simultaneously in several cultures. Additionally, we sequenced transcriptomes of four 2,000-generation strains and found a surprising long-term reversal of the short-term benzoate stress response. We report the effects of several candidate gene deletions and mutations on fitness in the presence of benzoate and of chloramphenicol.

RESULTS

Early benzoate-selected mutations affect Gad, Mar and aromatic metabolism. We sought to assess the timeline of benzoate-tolerance evolution, and identify genes that acquired mutations early, without the context of preexisting mutations (18). We isolated clones from frozen populations ancestral to those published for generation 2,000 (**Table 1**). Colonies were obtained on LBK agar from frozen populations corresponding to generations 900 and 1,400, for the microplate well populations A1, A5, C3, and G5. These populations at generation 2,000 had produced isolates A1-1, A5-1, C3-1, G5-1, and G5-2; these key strains are benzoate-tolerant, and all except G5-1 are more sensitive to chloramphenicol than the ancestor (18). Selected isolates were sequenced (**Table S1**), and mutations were detected using *breseq* (46). Mutations for selected strains are listed in **Table 2**, alongside the mutations from generation 2,000 clones (18). All mutations for all clones sequenced are compiled in **Table S2**.

The early-generation clones (900 or 1,400) were tested for adaptation to growth in 20 mM benzoate (**Fig. 2**). At this benzoate concentration, the ancestral strain W3110 starts to grow but then fails and commences decline at approximately 12 h (18). All the A1 population strains from generation 900 or 1,400 grew to stationary phase in 20 mM benzoate. From the A5 population, only the A5-5 strain (generation 1,400) achieved a sustained endpoint. In population G5, all the early isolates grew well (G5-3, G5-4, G5-5); but in population C3, the generation 900 strains grew only slightly better than W3110. Overall, the various early-generation isolates showed differing rates of adaptation to benzoate.

Clones frozen before generation 1,000 had several mutations that persisted in strains at generation 2,000 (**Table 2**). Three of these affected Gad regulation: the partial Gad island deletion *ΔmdtE-slp* (all isolates from population A1), the Gad activator *ariR* (population A1)

(47), and GadE-activator *gadX* (population A5). In fact, more than half the isolates sequenced had one of seven different mutations within the *slp-gad* island (**Table S1**). Large deletions were mediated by upstream insertion sequences, a common finding in stress evolution experiments (18, 45). Thus our early-generation sequences confirmed that loss of Gad acid resistance was strongly selected by benzoate.

Loss of the Gad regulon, either by deletion or downregulation, includes loss of the MdtEF-TolC efflux pump, which is specifically upregulated by GadX (30). MdtEF-TolC exports a variety of antibiotics and toxic metabolites, including chloramphenicol (40, 48, 49). It is one of a number of MDR pumps and regulators reported to be lost or mutated in genomes evolved with benzoate (18) or with CCCP (20). Note that while *mdtEF* mutations did appear early, sensitivity to chloramphenicol was not detected before generation 1,400 or 2,000 (**Table 2**). This suggests that multiple mutations accumulate over generations contributing to the phenotype.

Other genes that had early, persistent mutations include *folD* (5,10-methylene-tetrahydrofolate dehydrogenase/cyclohydrolase, for thymidine biosynthesis) (50) in population A1; and *apt* (adenosine phosphoribosyltransferase, for purine salvage) (51) in population A5. A 6-bp insertion upstream of *apt* was found by generation 500 in population A5 and persisted through generation 2,000; and a frameshift in *apt* coding sequence was in strain E1-5 (**Table S2**). Overall, various isolates had mutations affecting metabolism of nucleotides and aromatic amino acids. Strain E1-5, generation 1,000, had a mutation in *yeaS* (*leuE*) whose product effluxes leucine and toxic analogues. Biosynthetic genes included *aroF* (3-deoxy-d-arabino-heptulosonate 7-phosphate synthase; first step of tyrosine biosynthesis) (52) and *hisG* (ATP-phosphoribosyltransferase, first step of histidine biosynthesis) (53);. Other mutations affected aromatic catabolism and salvage: *add* (adenosine deaminase) (54); *deoD* (PNP, purine

nucleoside phosphorylase) (55); *rihA* (ribonucleoside hydrolase) (56); *paaE* (phenylacetate degradation) (57); and *nupG* (nucleoside uptake transporter, PMF-driven) (58). These mutations in aromatic metabolism may represent adjustment to the uptake of benzoate in the cytoplasm. These effects may be associated with the proposed induction of Mar regulon by intracellular aromatic intermediates that retard growth above a certain level (59, 60).

Transcriptome of benzoate-evolved isolates shows reversal of benzoate regulation in the ancestor W3110. In our previous study of acid stress, the transcriptomes of acid-evolved clones compared to those of the ancestor proved highly informative, revealing the surprising knock-down of several acid stress genes (22). We therefore conducted a similar transcriptome analysis of our benzoate-evolved strains (18), and of the ancestral strain under benzoate and no-benzoate conditions. Four of the 2000-generation strains were selected (A1-1, C3-1, G5-1, and G5-2). RNA was extracted during logarithmic growth from cultures supplemented with a relatively modest benzoate stress (5 mM benzoate) in order to sustain comparable growth levels of all strains. In addition, the ancestor W3110 was cultured in medium with or without 5 mM benzoate, in order to identify genes responding to benzoate stress before benzoate selection occurred.

Figure 3 plots the $\log_2$ expression ratios (versus ancestor) for each benzoate-evolved 2000-generation strain against the $\log_2$ ratios for expression in the ancestor, with benzoate versus without. Remarkably, across the genome, genes that were regulated up or down by benzoate in the ancestor showed reversal (by knock-down or by deletion) in the four independently evolved isolates. In some cases, the reversal involved deletion of several genes or a major regulator, such as the deletion of nearly the entire Gad island *slp*-[*gadW*] in A1-1, or loss of the *gadX* activator in G5-1 and in G5-2. These strains showed absence or knock-down of most of the Gad regulon

(blue symbols in **Figure 3**). But strain C3-1 also had knockdown of Gad, despite no loss of known regulators.

The $\log_2$ expression ratios for individual genes of strain W3110 in the presence or absence of benzoate are presented in **Table S3**. Genes are shown for ratios ≥2 ($\log_2$ ratios ≥1) with significance at a value of $p \leq 0.01$. Expression ratios are also shown for the 2,000-generation strains versus W3110, cultured in benzoate. Selected differentially expressed genes are shown in **Table 3**.

In W3110, benzoate upregulated much of the Gad regulon including both glutamate decarboxylases (*gadA*, *gadB*) and glutamate transporter *gadC*, the regulator *gadE*, and the gad-associated multidrug efflux pump *mdtEF*. The *hdeABD* portion of the Gad island showed less induction because *hdeAB* is repressed by MarA (**Fig. 1**) which is induced by benzoate (**Table 3**). Benzoate induction of glutamate decarboxylase would be consistent with Foster's model that cytoplasmic pH depression induces Gad (61). However, the cytoplasmic pH depression caused by benzoate uptake does not involve extreme acidification of the periplasm. Thus, there is less need for periplasmic chaperones HdeA and HdeB.

While MarA is induced by benzoate in the ancestor, the benzoate-evolved strains show various losses of mar regulon components, either by *marRAB* deletion (strain A5-1, **Table 2**) or by loss of another regulator such as *rob* (strain G5-2). MarA mediates downregulation of the large outer membrane porin, *ompF* (**Fig. 1**). The downregulation of *ompF* helps exclude toxins and antibiotics. No *ompF* mutations appear in our evolved strains, yet two of the four benzoate-evolved strains (A1-1 and G5-2) showed upregulation of *ompF*. Strain C3-1 upregulated two other large porins, *ompG* (62) and *phoE* (63) as well as *ompL* (64). Strain G5-1 upregulated porins *phoE* and *ompL*. Thus, under long-term exposure to benzoate, with concomitant PMF

depletion, all four strains upregulated porins that could enhance fitness by admitting more carbon sources for substrate-level phosphorylation. The porins could also increase sensitivity to antibiotics in the benzoate-evolved strains.

The genes induced by benzoate also included several components of electron transport, including cytochrome *bo*$_3$ ubiquinol oxidase (*cyoABCDE*), cytochrome oxidase *bd-II* (*appBC*) (65, 66), nitrate reductase (*narHJ*) (67), and hydrogenase-3 (Hyd-3, *hycABCDEFG*) (68). Hyd-3 converts H^+ ions to H_2, and associates with the formate-hydrogenlyase complex (FHL); it includes HycA regulator of FHL (69). The acceleration of electron transport is consistent with the effect of uncouplers on respiration, generating a futile cycle during stationary phase (70). The energy loss during stationary phase could explain why strain W3110 enters death phase after several hours in culture with 20 mM benzoate (18).

All four of the benzoate-evolved strains had knocked down expression of FHL/Hyd-3 components (*hyc* genes), and strain A1-1 showed decrease of *appBC* cytochrome oxidase *bd-II*. All these complexes--Hyd-3, FHL-3, and the *bd-II* oxidase--are generally expressed under low-oxygen conditions (68, 71). Hyd-3 converts $2H^+$ to H_2, as part of the formate-hydrogen lyase complex converting formate to CO_2 plus H_2 (72). Hydrogen production by Hyd-3 is induced by external acid, and is required for extreme-acid survival in low oxygen (73). Thus the benzoate-associated loss of acid-inducible hydrogenase (and presumably FHL) parallels the loss of the acid-inducible Gad system.

No hydrogenases show mutations in our resequenced genomes, although three different mutations appear affecting the nitrate-inducible formate dehydrogenase (*fdnG* and *fdnI*) (74). Also in A1-1, the *narGHI* quinol-nitrate oxidoreductase (75) is down-regulated. Thus some kinds of reregulation have occurred that decrease the wasteful expenditure of electrons. These changes

most likely enable benzoate adaptation during the low-oxygen period of stationary phase, the period in which the ancestral strain declines (**Fig. 2**).

Deletion of *gadE*, *mdtE*, *mdtF*, or *ariR* confers benzoate tolerance. Our resequenced genomes of benzoate-evolved strains offered candidate genes for mechanisms of benzoate tolerance. We started with the isolates from population A1, which suggest a progression of acquired mutations that contribute to benzoate tolerance. The early-generation isolates do not necessarily represent direct ancestors of the later strains, yet the *slp-gadX* deletion is present in all A1 strains sequenced, and this region encompasses most early mutations found in other populations (**Table 2**). We constructed, by recombineering (76), a strain with a deletion spanning the start of *slp* to the end of *gadX* (*slp-gadX* strain).

For comparison, strains were cultured in microtiter plates with 15 mM benzoate, as described under Methods (**Fig. 4**). Endpoint growth was measured at 16 h; and for each condition, we show a replicate curve with median 16-h OD_{600}. The *slp-gadX* strain had higher 16-h growth relative to W3110, and nearly as high as that of the benzoate-evolved strain A1-1 (**Fig. 4A**). W3110 mutants deleted for *gadE* or *gadX* did not show a consisted effect on growth, although their regulation of the Gad island (61) could have fitness effects detectable by direct competion.

The ancestor W3110, and our benzoate-evolved strains, show growth effects of salicylate that are comparable to the effects of benzoate, at lower concentration (18). An experiment similar to that of Figure 4B was conducted using chloramphenicol with 2 mM sodium salicylate instead of 5 mM benzoate; similar results were obtained. **Figure S1** presents salicylate experiments comparable to all the 5 mM benzoate experiments in Figures 4, 5, 6.

We then tested the benzoate tolerance of strains deleted for the *mdtE* and *mdtF* components of the MdtEF-TolC MDR efflux pump, which is included in the acid fitness island deletion. Knockout strains of *mdtE*::*kanR* and *mdtF*::*kanR* each had increased growth rate and 16-h density relative to W3110 in 15 mM benzoate at pH 6.5 (**Fig. 4C**). The increase was however significantly less than that found for strain A1-1. This suggests that various genes of the Gad system make additive partial contributions to benzoate tolerance.

Another mutation in A1-1 that had the potential to affect benzoate tolerance including a transposon-mediated knockout of *ariR* (18, 39). A KEIO *ariR*::*kanR* deletion strain had increased endpoint growth compared to wild-type. AriR (YmgB) regulates both Gad acid resistance and biofilm formation (39) possibly mediated by RpoS (77). We tested whether an *ariR* deletion interacted with the acid fitness island deletion in an additive manner, or was overshadowed by the larger deletion. We transduced *ariR*::*kanR* into the *slp-gadX* strain (**Fig. 4E**). This strain grew identically to the *slp-gadX* strain in 15 mM benzoate. No *ariR* mutation was detected in the sequence of the 500-generation isolate, so it appears likely that the *ariR* mutation in strain A1-1 has an additional contribution to benzoate tolerance that requires a more sensitive fitness assay for detection.

Chloramphenicol sensitivity is conferred by *rpoA* K271Q but not by *slp-gadX* deletion. Benzoate tolerance of our benzoate-evolved strains is associated with a tradeoff of sensitivity to chloramphenicol, as seen for strains A1-1, A5-1, C3-1, G5-1, and G5-2 (18). The basis of this tradeoff is unknown. Our new isolates from the early generations confirmed that chloramphenicol sensitivity emerged later than benzoate tolerance; only one generation 1,400 isolate (A1-5) and none of the earlier isolates showed measurable decrease in growth with chloramphenicol, at 4µg/ml or at 8µg/ml (**Table 2**, second row). The *slp-gadX* deletion and

deletions of individual genes were also tested for their effects on chloramphenicol resistance (**Fig. 4B, D, F**). Chloramphenicol resistance was tested in a medium containing a low level of benzoate (5 mM) in order to induce any Mar and non-Mar MDR systems. None of the mutations affected chloramphenicol resistance, despite the chloramphenicol efflux by MdtEF-TolC (49). This could occur because chloramphenicol is exported by redundant systems outside *slp-gadX*.

We hypothesized that the chloramphenicol sensitivity of strain A1-1 required an additional mutation acquired relatively late in the evolution experiment, perhaps between generations 900 and 1,400. An interesting candidate was the *rpoA* mutation that appeared in strain A1-5 (generation 1,400, chloramphenicol sensitive) and persisted in A1-1. The carboxy-terminal domain of this subunit regulates gene expression by interacting with upstream promoter elements, and transcription factors such as CRP. Our allele *rpoA* K271Q is nearly the same as a well-studied *rpoA* allele, *rpoA341* K271E (78, 79). The *rpoA341* allele downregulates certain positively-controlled regulons, such as *mel*, *ara*, and *cys*; but not all positive regulators are affected. The *rpoA341* allele may also upregulate loci such as *ompF* (78). We found *ompF* upregulated in strain A1-1 (**Table 3, Table S3**). Strain A1-1 also had knocked down expression of *araBAD* and of *cysA*, as reported for the *rpoA341* allele (78).

We sought to test the contribution of *rpoA* K271Q in strain A1-1 with respect to benzoate tolerance and chloramphenicol sensitivity. To do this, we replaced the mutant allele with $rpoA^+$ by co-transduction from W3110 into A1-1 using the linked marker *yhdN*::*kanR*. Strain JLS1616 (A1-1 Δ*yhdN*::*kanR* $rpoA^+$) was then cultured in parallel with strain A1-1 and the parent W3110 (**Fig. 5**). In 15 mM benzoate, the A1-1 $rpoA^+$ strain grew similarly to the parent A1-1, with no significant difference at any time point (panel A). However, with chloramphenicol and low benzoate (5 mM) the A1-1 $rpoA^+$ showed growth comparable to that of W3110, whereas A1-1

with the *rpoA* mutation was sensitive to chloramphenicol. Thus, *rpoA* K271Q is responsible for the loss of chloramphenicol resistance associated with benzoate evolution of A1-1.

Other alleles from the A1-5 strain (generation 1,400) are of interest, such as *rpoB* G373S. Commonly a mutation in an RNA polymerase subunit is followed by evolution of a second mutation that partly corrects the phenotoype; whether *rpoA* or *rpoB* mutated first, in this case, is unknown. Mutations also occurred in *fucA* (L-fuculose-1-phosphate aldolase) and in *cpxA* (stress two-component regulator), deletions of which had no effect on benzoate growth or chloramphenicol sensitivity, under our conditions tested. The gene mutations could however show effects under different conditions, or under competition selection. In competition assays with drug resistant strains, antibiotics typically show a minimum selective concentration (MSC) as much as 100-fold lower than the minimum inhibitory concentration (MIC) (80).

***cspC* deletion confers benzoate tolerance and *rfaY* confers chloramphenicol-sensitive growth rate.** In the C3-1 strain, there were two transposon-mediated deletions affecting growth in benzoate: a post-transcriptional regulator *cspC*, and the LPS kinase *rfaY*. The sequence of *cspC* is similar to that of other cold-shock proteins, and the CspC protein has been shown to upregulate genes under RpoS control by stabilizing the *rpoS* mRNA (81–83). A Δ*cspC*::*kanR* knockout strain showed increased growth relative to wild-type in 15 mM benzoate (**Fig. 6A**). However, in media with 4 µg/mL chloramphenicol, this strain grew identically to wild-type (**Fig. 6B**).

An Δ*rfaY*::*kanR* strain showed no phenotype in 15 mM benzoate (**Fig. 6A**). The double mutant Δ*cspC*::*kanR* Δ*rfaY*::*kanR* grew identically to the Δ*cspC* strain. In chloramphenicol however, Δ*rfaY*::*kanR* had a mean growth rate of 0.12 ± 0.01 doublings per hour in early log phase, which was less than the mean W3110 growth rate of 0.39 ± 0.02 doublings per hour (**Fig.**

6C). A t-test comparison gave a p-value of $p < 0.01$. The double mutant also showed a significant decrease in growth rate, compared to Δ*cspC*::*kanR.* Thus, the double mutant showed the *cspC* phenotype cultured in 15 mM benzoate but the *rfaY* phenotype cultured with chloramphenicol (5 mM benzoate).

The C3 population isolates had no mutations within *slp-gadX*, except for a *gadX* knockout in C3-5. Yet strain C3-1 had knocked down transcription of *gadABC* (**Fig. 3**) so its genome must have altered regulation of acid-tolerance pathways. Given that *cspC* is implicated in the stabilization of the *rpoS* mRNA (82, 84) it is possible that *cspC* deletion downregulates Gad, via decreased RpoS concentration (**Fig. 1**). Unlike the A1 and A5 populations, the sequenced isolates from C3 populations showed little evidence of shared ancestry. It is possible that these populations contained multiple sub-populations of different ancestry with similar fitness. During the isolation process, different sub-populations were sampled at each time-point, one of which could have taken over the well at some point between generation 1,400 and generation 2,000, and this population's descendent resulted in the generation 2,000 isolate.

***emrA* deletion confers benzoate tolerance.** In G5 (strain G5-3, G5-4), a 6,012 bp deletion was present in the Gad island, although not detected in our later generation isolates. As seen for population C3, population G5 shows evidence of independent subpopulations (**Table 2**). Strains G5-5 and G5-1 have a knockout mutation in *emrA,* which normally encodes part of the EmrAB-TolC pump (19). The *emrA* gene acquires point mutations--but not knockouts--under evolution with the uncoupler CCCP, which is expelled by EmrAB-TolC (20). Deletion of *emrA* conferred a degree of tolerance to benzoate (**Fig. 7A**) even in the presence of chloramphenicol (**Fig. 7B**).

***add* deletion confers benzoate tolerance and *rob* confers chloramphenicol sensitivity.**

Strain G5-2 contains a frameshift in *add*, a gene encoding adenosine deaminase which catalyzes a proton-consuming reaction of purine catabolism that protects the cell from acid by a mechanism analogous to that of GadA (85). Deletion of *add* conferred partial tolerance to benzoate (**Fig. 7C**). This result is yet another example of benzoate selection against an external-acid protection mechanism.

G5-2 also contains a point mutation in *rob* encoding a MarA-type regulator that enhances chloramphenicol resistance (41). Deletion of *rob* did not significantly enhance growth in 15 mM benzoate (**Fig. 7C**). The *Δrob* did however decrease the log-phase growth rate in chloramphenicol, from an average W3110 growth rate of 0.63 ± 0.01 doublings per hour to an average growth rate of 0.59 ± 0.02 doublings per hour for *Δrob* (**Fig. 7E**). A t-test comparison gave a p-value of $p < 0.01$. Replicates for the log-phage growth region are shown for *Δrob* and W3110 in 4 µg/ml chloramphenicol (**Fig. 7E**).

Hydrogenase 3 deletion enhances late growth. Our transcriptomes showed benzoate induction of hydrogenase 3 in W3110, yet knockdown of *hycEFG* in all four benzoate-evolved strains (**Table 3**). We tested the growth of W3110 strains deleted for *hycE* (encoding the hydrogenase activity, $2H^+ \rightarrow H_2$) and *hycF* (subunit of formate hydrogenlyase complex) (86). Both *ΔhycE*::*kanR* and *ΔhycF*::*kanR* strains reached higher OD_{600} than did W3110 during late growth, measured at 20 h (**Fig. 8**). These results confirm that although benzoate exposure induces consumption of cytoplasmic protons via hydrogenase 3, as part of formate breakdown, this activity decreases long-term relative fitness in benzoate. Hydrogenase 1 (*hya*) consumes H_2, producing $2H^+$ (68). The hydrogenase 1 deletion *ΔhyaB*::*kanR* showed no significant difference from W3110.

Other genes tested. KanR knockout strains were tested for other genes that had mutant alleles in our benzoate-evolved isolates, but no significant difference from the ancestor was detected for growth with benzoate or with chloramphenicol. As noted, such differences might emerge under extended direct competition. The genes tested by 22 h culture with 15 mM benzoate include: *acnA*, *chbC*, *cpxA*, *deaD*, *fucA*, *mdtA*, *gltP*, *hdeD*, *pepN*, *rnb*, *yhfM*, *uxaA*, and *yhiD*.

DISCUSSION

Here we have combined genomic, transcriptomic, and genetic approaches to study how *E. coli* evolve in the presence of benzoic acid at pH 6.5 (18). Our work extends the picture of known MDR-related genes mutated under exposure to partitial or full uncouplers (20) and suggests additional mechanisms for the increased sensitivitiy to antibiotics, such as the upregulation of porins. This subject has implications beyond *E. coli*, as the microbiomes of soil and rhizosphere (87) as well as human and animal digestive tracts (88) are exposed to benzoate and related compounds.

Evolution with benzoate reverses short-term benzoate regulation. Previously we showed that evolution with benzoate incurs frequent mutations of the Gad acid fitness island (18). Similarly, evolution at low pH has the counterintuitive result of deletion or knock-down of highly expressed acid resistance mechanisms including Gad as well as lysine and arginine decarboxylases (21). Our transcriptomes extend the benzoate result reveal a striking pattern of knockdown of Gad as well as many other benzoate-inducible gene products in the benzoate-evolved strains (**Table 3**). Even a strain with no mutations in the fitness island (C3-1) had knock-down of Gad, possibly by mutation of the RpoS post-transcriptional activator CspC. This result reflects a pattern of convergent evolution achieved via one of several possible genetic histories.

The reversal of short-term stress response after long-term exposure to acids may reflect a more general tendency for experimental evolution to restore global pre-stress conditions. An analogous effect was reported after heat-stress evolution of *E. coli*, where the resulting strains show loss of heat shock gene expression (89). Another example is that of experimental evolution in glycerol or lactate minimal media, where expression of many genes ultimately returns to pre-stress levels (90). The fitness cost of stress response could involve either the cost of stress-

induced gene expression, when it fails to provide a benefit (21); or the cost of excess PMF expenditure by a transporter or an efflux pump (24).

A striking example of benzoate regulation reversal was the knockdown of hydrogenase 3 (**Table 3, Fig. 8**). Hyd-3 as part of formate hydrogenlyase complex normally converts formate from fermentation to CO_2 and H_2. Yet we show that in the presence of benzoate, Hyd-3 deletion enhances fitness during late stationary phase, the period where we would expect FHL/Hyd-3 to be active (71). There is evidence that FHL activity exports protons (91). If so, this could be yet another system that wastes energy as exported protons drive benzoate into the cell—and thus decreases relative fitness over long-term subculturing. The possible effects of benzoate and other partial uncouplers could be relevant to the biotechnology of hydrogen production (86).

In strain A1-1, several alternative terminal oxidases were knocked down. Antibiotic resistance is linked to bacterial respiration, as several bactericidal antibiotics are shown to increase respiratory rates, while most bacteriostatic compounds decrease respiration (92). One means of adaptation to high benzoate concentration could be to limit respiration by down-regulating unneeded components of electron transport, including anaerobic respiration. This would limit the energy wasted by uncoupling respiration from ATP synthase. Introduction of antibiotics to a respiration-compromised cell could amplify the phenotype, and lead to benzoate-induced antibiotic sensitivity.

The benzoate induction of Mar regulon also shows various forms of reversal after prolonged benzoate exposure. MarA downregulates the OmpF porin, presumably in order to exclude antibiotics. But long-term benzoate exposure increases expression of several large-hole porins (OmpF, OmpG, PhoE, OmpL). This finding would be consistent with a tendency to

decrease PMF dependence while amplifying access to fermentable carbon sources for substrate-level phosphorylation.

Deletion analysis reveals contributors to benzoate tolerance and chloramphenicol sensitivity. Several components of the *slp-gadX* island lead to benzoate tolerance. Loss of MdtEF-TolC drug efflux system directly increases benzoate tolerance. This efflux pump couples drug efflux to PMF (27, 29, 93). The increase of benzoate tolerance in *mdtEF* knockout strains could result from a decrease of PMF stress. Theoretically, benzoate induces a PMF stress by shuttling protons through the membrane (18). Thus, the presence of other proteins that utilize PMF further depletes the pool of extracellular protons available for core cell processes. It is possible that deleting drug efflux systems reduces proton flux through systems with functions that do not increase fitness in benzoate, leading to antibiotic sensitivity. Loss of regulators such as *gadE* may decrease activation of *mdtEF*, but also may relate to regulatory connections outside the Gad island (16, 25, 31, 93, 94).

Here we have shown three candidate alleles associated with antibiotic sensitivity, namely, the *rpoA* mutation in A1-1; the *rfaY* mutation in C3-1, and the *rob* mutation in G5-2. Since the mutation in *rpoA* is in the carboxy-terminal domain, which interacts with UP-elements and certain transcription factors, it is possible that this mutation down-regulates a large set of genes (95, 96). This down-regulation could free up resources for response to benzoate stress, which could include a large number of PMF-driven antibiotic resistance genes. In fact, there is previous evidence suggesting that an interaction between the CTD of RpoA and MarA is necessary for the antibiotic resistance activator to function (96). By mutating the RpoA CTD, the antibiotic-resistance properties of MarA could be lost without affecting *marA* transcription. Less clear is how the *rfaY* mutation both contributes to benzoate tolerance and/or antibiotic sensitivity. This

gene encodes a membrane-bound enzyme that phosphorylates the inner core of lipopolysaccharide (LPS), a function which has been implicated in membrane stability (97). Decreased membrane stability caused by the *rfaY* mutation may increase the permeability of certain antibiotics, thereby decreasing C3-1's antibiotic resistance.

Another surprising finding was the pervasive occurrence of small mutations in genes for aromatic biosynthesis and catabolism, such as *folD* and *add.* The *folD* gene is essential and could not be deleted, but deletion of *add* was shown to enhance benzoate tolerance. The evidence points to further exploration of the role of benzoate and salicylate in modulating efflux of aromatic intermediates of metabolism (59) especially given the benzoate-evolved enhancement of substrate influx via porins (**Table 2).**

Note that the relative fitness advantage of a given allele can accrue by various means at different phases of the growth cycle. Most of the candidate genes we tested, such as *gadE*, *mdtE*, and *cspC*, enabled cells to grow to a higher optical density than the parent W3110. However, the chloramphenicol sensitivity associated with some alleles, such as *rfaY*, was caused by slower rate of growth during log phase. While the bacteria grew to an optical density comparable to that of W3110, had the two strains been competing in co-culture, the mutant strain would have soon lost out to the parent.

Overall, we reveal genetic mechanisms by which multigenerational exposure to benzoate leads to increased tolerance of benzoate or salicylate, with the tradeoff of sensitivity to certain antibiotics. Our findings have implications for the role of benzoate as a food preservative, and salicylate as a plant defense agent and as a therapeutic substance for long-term use.

METHODS

Bacterial strains and culture conditions. *E. coli* K12 W3110 (Laboratory stock D13) was the parent for all genetic analysis. The strain was resequenced for analysis (18). Unless otherwise specified, bacteria were cultured in LBK (10 g/L tryptone, 5 g/L yeast extract, 7.45 g/L KCL) with a pH buffer, at 37 °C. Growth media were supplemented with benzoate, salicylate, kanamycin (50 ug/ml), or chloramphenicol (4 or 8 ug/ml) as necessary. For growth curves, media was buffered to pH 7.0 with 100 mM (3-(*N*-morpholino)propanesulfonic acid) (MOPS; pKa = 7.20) or to pH 6.5 with 100 mM piperazine-N,N′-bis(2-ethanesulfonic acid) (PIPES; pKa = 5.96), containing 70 mM Na^+. The media pH was adjusted with either 5 M HCL or 5 M KOH. Cultures were incubated at 37˚C unless otherwise specified. Strains with *kanR* insertions were obtained from the Keio collection (98). The XTL241 strain containing the *cat-sacB* fusion was obtained from the Court lab at NCI (76). All other strains used in this study are derived from W3110 and listed in **Table 1**, and in **Table S1** (new isolates with resequenced genomes).

Growth Curves. For growth curves in 15 mM benzoate, strains were cultured overnight in LBK 100 mM PIPES pH 6.5 supplemented with 5 mM benzoate. These cultures were diluted 1:200 in a 96-well plate into fresh LBK buffered to pH 6.5 with 100 mM PIPES supplemented with 15 mM benzoate. OD_{600} was read in a Spectramax spectrophotometer every 15 min for 22 h. For growth curves in chloramphenicol, strains were cultured overnight in LBK 100 mM MOPS pH 7 supplemented with 5 mM benzoate as needed. These cultures were diluted 1:100 into fresh media supplemented with 4 ug/ml chloramphenicol, unless stated otherwise. Endpoint OD_{600} was defined as the cell density after 16 h. Significance tests included ANOVA with Tukey's post-hoc test (R software). Each data figure represents three experiments in each of which 8 replicate cultures were tested, unless stated otherwise.

Genome sequencing of early generation evolved-strains. Genomic DNA from early-generation clones and from the ancestral stock W3110 was extracted with a DNeasy DNA extraction kit (Qiagen) and a MasterPure Complete DNA and RNA purification kit (Epicentre, WI). Purity was determined by Nanodrop 2000 spectrophotometer (Thermo Fisher Scientific), and concentration was determined by Qubit 3.0 fluorometer (Thermo Fisher Scientific).

Genomic DNA was sequenced on an Illumina Mi-seq platform, at the Michigan State University Research Technology Support Facility Genomics Core. Libraries were prepared with an Illumina TruSeq Nano DNA library preparation kit. After library validation and quantitation, libraries were pooled and loaded on an Illumina MiSeq flow cell. Sequencing was performed in a 2 by 250-bp paired-end format with an Illumina 500 cycle V2 reagent cartridge. Base calling was performed by Illumina Real Time Analysis v1.18.54, and the output of RTA was demultiplexed and converved to FastQ format with Illumina Bcl2fastq v1.8.4. Mutations were called by alignment to the *E. coli* W3110 reference NC_007779.1 using the *breseq* computational pipeline (46).

Strain construction. *E. coli* W3110 strains were constructed by P1 transduction and by recombineering. P1 transduction was performed by standard methods (99). Strains carrying *kanR* resistance cassettes in genes of interest were acquired from the Keio collection (98).

The *gadX-slp* strain (JLS1726) was constructed using lambda-red recombineering according to the protocol by Thomason (76). Generation of the acid fitness island knockout strain, JLS1726, was performed using λ recombineering with the protocol described by Thomason *et al*, 2014. Overnight cultures of E. coli with the pSIM6::*ampR* plasmid were diluted 1 to 70 in LB (5 g/L NaCl) and grown to mid log-phase (OD600 between 0.4 and 0.6) in a shaker flask at 32°C. A 15 mL aliquot of this subculture was transferred to a fresh flask and shaken at

42 °C for 15 min. Cells were made electro-competent and electroporated with a DNA oligonucleotide. Cells were outgrown at 32°C for 3 to 5 hours, and plated onto selective media. For construction of JLS1726 (Δ*slp*-Δ*gadX*), a dsDNA oligo containing a cat-sacB (chloramphenicol resistance – sucrose sensitivity selection/counter-selection marker) with 50 bp of homology to slp and 50 bp of homology to *gadX* was constructed using the *cat-sacB* hybrid primers listed in Table 2.Then, this region was replaced with the 70 bp oligo, aaacagtaatatgtttatgtaatattaagtcaactaatagatatttctttatagttttcatctgattctg, to produce a strain with a clean break at the start of *slp* and end of *gadX*.

Transcriptome analysis. The transcriptomes of evolved isolates in comparison with ancestor were obtained as for Ref (22). For RNA extraction, bacteria were cultured to stationary phase in LBK buffered to pH 6.5 with 100 mM PIPES at 37°C. Cultures were diluted 1:50 into fresh medium supplemented with 5 mM potassium benzoate, and grown to early log phase (determined by OD_{600} of 0.4). At mid-log phase (OD600 between 0.4 and 0.6), cultures were diluted 6:1 into 5% phenol-ethanol solution and pelleted. The pellet was resuspended in TE buffer (100 µL) with 3 mg/ml lysozyme, as described by He *et al* (22). A Qiagen RNeasy minikit was used to further purify RNA. An additional DNase treatment (MoBio DNase-Max) was conducted.

Illumina RNA-Seq libraries were constructed for sequencing. An enrichment of messenger RNA was achieved by depleting ribosomal RNA (rRNA) by following the guidelines of the Ribo-Zero rRNA Removal Kit (Illumina)(22, 100). The RNA-Seq library was prepared via the ScriptSeq v2 RNA-Seq library preparation kit (Epicenter, WI) with a starting concentration of 15 ng rRNA depleted RNA for each library. The resulting random-primed cDNA was purified with the MinElute PCR Purification Kit (Qiagen) before the 12 PCR cycle amplification step

using the FailSafe PCR enzyme kit (Epicenter,WI) and selected ScriptSeq Index primers as reverse primers. The Agencourt AMPure XP system (BeckmanCoulter, NJ) purified the libraries and thereby size selected for > 200 bp. Each library's size and quality was assessed on the Agilent 2100 Bioanalyzer and a High Sensitivity DNA Chip (Agilent Technologies, Wilmington, DE) and quantified with the NEBNext Library Quant Kit Protocol (New England BioLabs). The NextSeq 500/550 High Output Kit (300 cycles) was used for sequencing using the The Illumina NextSeq 500. (61)

Sequences were initially analyzed using CLC Genomics software, version 6.0. Sequences with a quality score of less than 30 were discarded, the remaining sequences were trimmed, and sequences of less than 36 bp were discarded. Sequences were mapped to the *E. coli* W3110 genome, (NCBI accession number NC_007779.1) using the following CLC genomics mapping parameters: mismatch, 1; insertion, 3; deletion, 3; length, 0.9; similarity, 0.95; auto-detect paired distances on and map randomly. CLC RNA-seq was performed using the following parameters: mismatch, 2; length fraction, 0.9; similarity fraction, 0.95; strand specific selected; maximum 3 hits, 3; paired settings, 36 to 500; broken pairs counting selected. Only unique counts generated for individual genes were used as the starting data for all subsequent analyses.

Differential expression analysis was performed using the R package DESeq2. Reported log-fold-changes represent difference in expression of each gene in the evolved strains in 5 mM benzoate relative to the ancestor in the same condition. We also performed a control comparing the ancestor in 5 mM benzoate to the ancestor without benzoate. A gene was said to be differentially expressed if it had a log-fold-change greater than 1, and p-value < 0.001.

Accession numbers for resequenced genomes and for RNAseq. The SRA accession number for RNAseq files is: PRJNA491479.

ACKNOWLEDGMENTS

This work was supported by award MCB-1613278 from the National Science Foundation and by Summer Science funds from Kenyon College.

REFERENCES

1. Macfarlane GT, Macfarlane S. 2011. Fermentation in the human large intestine: Its physiologic consequences and the potential contribution of prebiotics. J Clin Gastroenterol 45:S120–S127.
2. Krulwich TA, Sachs G, Padan E. 2011. Molecular aspects of bacterial pH sensing and homeostasis. Nat Rev Microbiol 9:330–343.
3. Diez-Gonzalez F, Russell JB. 1999. Factors affecting the extreme acid resistance of *Escherichia coli* O157:H7. Food Microbiol 16:367–374.
4. Roe AJ, McLaggan D, Davidson I, O'Byrne C, Booth IR. 1998. Perturbation of anion balance during inhibition of growth of *Escherichia coli* by weak acids. J Bacteriol 180:767–772.
5. Terada H. 1990. Uncouplers of oxidative phosphorylation. Environ Health Perspect 87:213–218.
6. Lewis K, Naroditskaya V, Ferrante A, Fokina I. 1994. Bacterial resistance to uncouplers. J Bioenerg Biomembr 26:639–646.
7. Barker JL, Levitan H. 1975. Mitochondrial uncoupling agents - Effects on membrane permeability of molluscan neurons. J Membr Biol 25:361–380.
8. Gutknecht J. 1990. Salicylates and proton transport through lipid bilayer membranes: A model for salicylate-induced uncoupling and swelling in mitochondria. J Membr Biol 115:253–260.
9. Brul S, Coote P. 1999. Preservative agents in foods: Mode of action and microbial resistance mechanisms. Int J Food Microbiol 50:1–17.
10. Beales N. 2004. Adaptation of microorganisms to cold temperatures, weak acid

preservatives, low pH, and osmotic stress: A review. Compr Rev Food Sci Food Saf 3:1–20.

11. An C, Mou Z. 2011. Salicylic acid and its function in plant immunity. J Integr Plant Biol 53:412–428.

12. White RF. 1979. Acetylsalicylic acid (aspirin) induces resistance to tobacco mosaic virus in tobacco. Virology 99:410–412.

13. Doornbos RF, Van Loon LC, Bakker PAHM. 2012. Impact of root exudates and plant defense signaling on bacterial communities in the rhizosphere. A review. Agron Sustain Dev 32:227–243.

14. Barbosa TM, Levy SB. 2000. Differential expression of over 60 chromosomal genes in *Escherichia coli* by constitutive expression of MarA. J Bacteriol 182:3467–3474.

15. Cohen SP, Levy SB, Foulds J, Rosner JL. 1993. Salicylate induction of antibiotic resistance in *Escherichia coli*: Activation of the *mar* operon and a *mar*-independent pathway. J Bacteriol 175:7856–7862.

16. Mates AK, Sayed AK, Foster JW. 2007. Products of the *Escherichia coli* acid fitness island attenuate metabolite stress at extremely low pH and mediate a cell density-dependent acid resistance. J Bacteriol 189:2759–2768.

17. Ruiz C, McMurry LM, Levy SB. 2008. Role of the multidrug resistance regulator MarA in global regulation of the *hdeAB* acid resistance operon in *Escherichia coli*. J Bacteriol 190:1290–1297.

18. Creamer KE, Ditmars FS, Basting PJ, Kunka KS, Hamdallah IN, Bush SP, Scott Z, He A, Penix SR, Gonzales AS, Eder EK, Camperchioli DW, Berndt A, Clark MW, Rouhier KA, Slonczewski JL. 2017. Benzoate- and salicylate-tolerant strains of *Escherichia coli* K-12

lose antibiotic resistance during laboratory evolution. Appl Environ Microbiol 83:e02736.

19. Lomovskaya O, Lewis K, Matin A. 1995. EmrR is a negative regulator of the *Escherichia coli* multidrug resistance pump EmrAB. J Bacteriol 177:2328–2334.

20. Griffith JM, Basting PJ, Bischof KM, Wrona EP, Kunka KS, Tancredi AC, Moore JP, Hyman MRL, Slonczewski JL. 2019. Experimental evolution of *Escherichia coli* K-12 in the presence of PMF uncoupler CCCP selects for mutations affecting PMF-driven drug efflux pumps. Appl Environ Microbiol.

21. Dekel E, Alon U. 2005. Optimality and evolutionary tuning of the expression level of a protein. Nature 436:588–592.

22. He A, Penix SR, Basting PJ, Griffith JM, Creamer KE, Camperchioli D, Clark MW, Gonzales AS, Sebastian Chávez Erazo J, George NS, Bhagwat AA, Slonczewski JL. 2017. Acid evolution of *Escherichia coli* K-12 eliminates amino acid decarboxylases and reregulates catabolism. Appl Environ Microbiol 83:e00442.

23. Harden MM, He A, Creamer K, Clark MW, Hamdallah I, Martinez KA, Kresslein RL, Bush SP, Slonczewski JL. 2015. Acid-adapted strains of *Escherichia coli* K-12 obtained by experimental evolution. Appl Environ Microbiol 81:1932–1941.

24. Eames M, Kortemme T. 2012. Cost-benefit tradeoffs in engineered lac operons. Science 336:911–915.

25. Tramonti A, De Canio M, De Biase D. 2008. GadX/GadW-dependent regulation of the *Escherichia coli* acid fitness island: Transcriptional control at the *gadY-gadW* divergent promoters and identification of four novel 42 bp GadX/GadW-specific binding sites. Mol Microbiol 70:965–982.

26. Ruiz C, Levy SB. 2010. Many chromosomal genes modulate MarA-mediated multidrug

resistance in *Escherichia coli*. Antimicrob Agents Chemother 54:2125–2134.

27. Ma Z, Masuda N, Foster JW. 2004. Characterization of EvgAS-YdeO-GadE branched regulatory circuit governing glutamate-dependent acid resistance in *Escherichia coli*. J Bacteriol 186:7378–7389.

28. Ma Z, Gong S, Richard H, Tucker DL, Conway T, Foster JW. 2003. GadE (YhiE) activates glutamate decarboxylase-dependent acid resistance in *Escherichia coli* K-12. Mol Microbiol 49:1309–1320.

29. Hirakawa H, Inazumi Y, Senda Y, Kobayashi A, Hirata T, Nishino K, Yamaguchi A. 2006. N-acetyl-D-glucosamine induces the expression of multidrug exporter genes, *mdtEF*, via catabolite activation in *Escherichia coli*. J Bacteriol 188:5851–5858.

30. Nishino K, Senda Y, Yamaguchi A. 2008. The AraC-family regulator GadX enhances multidrug resistance in *Escherichia coli* by activating expression of *mdtEF* multidrug efflux genes. J Infect Chemother 14:23–29.

31. Tucker DL, Tucker N, Ma Z, Foster JW, Miranda RL, Cohen PS, Conway T. 2003. Genes of the GadX-GadW regulon in *Escherichia coli*. J Bacteriol 185:3190–3201.

32. Waterman SR, Small PLC. 2003. Transcriptional expression of *Escherichia coli* glutamate-dependent acid resistance genes *gadA* and *gadBC* in an *hns rpoS* mutant. J Bacteriol 185:4644–4647.

33. Borges-Walmsley MI, Beauchamp J, Kelly SM, Jumel K, Candlish D, Harding SE, Price NC, Walmsley AR. 2003. Identification of oligomerization and drug-binding domains of the membrane fusion protein EmrA. J Biol Chem 278:12903–12912.

34. Tanabe M, Szakonyi G, Brown KA, Henderson PJF, Nield J, Byrne B. 2009. The multidrug resistance efflux complex, EmrAB from *Escherichia coli* forms a dimer in vitro.

Biochem Biophys Res Commun 380:338–342.

35. Nagakubo S, Nishino K, Hirata T, Yamaguchi A. 2002. The putative response regulator BaeR stimulates multidrug resistance of *Escherichia coli* via a novel multidrug exporter system, MdtABC. J Bacteriol 184:4161–4167.

36. Kim HS, Nagore D, Nikaido H. 2010. Multidrug efflux pump MdtBC of *Escherichia coli* is active only as a B 2C heterotrimer. J Bacteriol 192:1377–1386.

37. Tanabe H, Yamasak K, Furue M, Yamamoto K, Katoh A, Yamamoto M, Yoshioka S, Tagami H, Aiba HA, Utsumi R. 1997. Growth phase-dependent transcription of *emrKY*, a homolog of multidrug efflux *emrAB* genes of *Escherichia coli*, is induced by tetracycline. J Gen Appl Microbiol 43:257–263.

38. Weatherspoon-Griffin N, Yang D, Kong W, Hua Z, Shi Y. 2014. The CpxR/CpxA two-component regulatory system up-regulates the multidrug resistance cascade to facilitate *Escherichia coli* resistance to a model antimicrobial peptide. J Biol Chem 289:32571–32582.

39. Lee J, Page R, García-Contreras R, Palermino JM, Zhang XS, Doshi O, Wood TK, Peti W. 2007. Structure and function of the *Escherichia coli* protein YmgB: A protein critical for biofilm formation and acid-resistance. J Mol Biol 373:11–26.

40. Deng Z, Shan Y, Pan Q, Gao X, Yan A. 2013. Anaerobic expression of the *gadE-mdtEF* multidrug efflux operon is primarily regulated by the two-component system ArcBA through antagonizing the H-NS mediated repression. Front Microbiol 4:194.

41. Duval V, Lister IM. 2014. MarA, SoxS and Rob of *Escherichia coli* – Global regulators of multidrug resistance, virulence and stress response. Int J Biotechnol Wellness Ind 2:101–124.

42. Sharma P, Haycocks JRJ, Middlemiss AD, Kettles RA, Sellars LE, Ricci V, Piddock LJV, Grainger DC. 2017. The multiple antibiotic resistance operon of enteric bacteria controls DNA repair and outer membrane integrity. Nat Commun 8:1444.

43. Bhaskarla C, Das M, Verma T, Kumar A, Mahadevan S, Nandi D. 2016. Roles of Lon protease and its substrate MarA during sodium salicylate-mediated growth reduction and antibiotic resistance in *Escherichia coli*. Microbiology 162:764–776.

44. Cohen SP, McMurry LM, Levy SB. 1988. *marA* locus causes decreased expression of OmpF porin in multiple-antibiotic-resistant (Mar) mutants of *Escherichia coli*. J Bacteriol 170:5416–5422.

45. He A, Penix SR, Basting PJ, Griffith JM, Creamer KE, Camperchioli D, Clark MW, Gonzales AS, Sebastian Chávez Erazo J, George NS, Bhagwat AA, Slonczewski JL. 2017. Acid evolution of *Escherichia coli* K-12 eliminates amino acid decarboxylases and reregulates catabolism. Appl Environ Microbiol 83:e00442.

46. Deatherage DE, Barrick JE. 2014. Identification of mutations in laboratory-evolved microbes from next-generation sequencing data using *breseq*. Methods Mol Biol 1151:165–188.

47. Tschowri N, Busse S, Hengge R. 2009. The BLUF-EAL protein YcgF acts as a direct anti-repressor in a blue-light response of *Escherichia coli*. Genes Dev 23:522–534.

48. Zhang Y, Xiao M, Horiyama T, Zhang Y, Li X, Nishino K, Yan A. 2011. The multidrug efflux pump MdtEF protects against nitrosative damage during the anaerobic respiration in *Escherichia coli*. J Biol Chem 286:26576–26584.

49. Bohnert JA, Schuster S, Fähnrich E, Trittler R, Kern W V. 2007. Altered spectrum of multidrug resistance associated with a single point mutation in the *Escherichia coli* RND-

type MDR efflux pump YhiV (MdtF). J Antimicrob Chemother 59:1216–1222.

50. Sah S, Aluri S, Rex K, Varshney U. 2015. One-carbon metabolic pathway rewiring in *Escherichia coli* reveals an evolutionary advantage of 10-formyltetrahydrofolate synthetase (Fhs) in survival under hypoxia. J Bacteriol 197:717–726.

51. Hershey H V., Taylor MW. 1986. Nucleotide sequence and deduced amino acid sequence of *Escherichia coli* adenine phosphoribosyl-transferase and comparison with other analogous enzymes. Gene 43:287–293.

52. Jossek R, Bongaerts J, Sprenger GA. 2001. Characterization of a new feedback-resistant 3-deoxy-D-arabino-heptulosonate 7-phosphate synthase AroF of *Escherichia coli*. FEMS Microbiol Lett 202:145–148.

53. Lohkamp B, McDermott G, Campbell SA, Coggins JR, Lapthorn AJ. 2004. The structure of *Escherichia coli* ATP-phosphoribosyltransferase: Identification of substrate binding sites and mode of AMP inhibition. J Mol Biol 336:131–144.

54. Chang ZY, Nygaard P, Chinault AC, Kellems RE. 1991. Deduced amino acid sequence of *Escherichia coli* adenosine deaminase reveals evolutionarily conserved amino acid residues: Implications for catalytic function. Biochemistry 30:2273–2280.

55. Koellner G, Bzowska A, Wielgus-Kutrowska B, Luić M, Steiner T, Saenger W, Stępiński J. 2002. Open and closed conformation of the *E. coli* purine nucleoside phosphorylase active center and implications for the catalytic mechanism. J Mol Biol 315:351–371.

56. Petersen C, Møller LB. 2001. The RihA, RihB, and RihC ribonucleoside hydrolases of *Escherichia coli*. J Biol Chem 276:884–894.

57. Teufel R, Mascaraque V, Ismail W, Voss M, Perera J, Eisenreich W, Haehnel W, Fuchs G. 2010. Bacterial phenylalanine and phenylacetate catabolic pathway revealed. Proc Natl

Acad Sci 107:14390–14395.

58. Xie H, Patching SG, Gallagher MP, Litherland GJ, Brough AR, Venter H, Yao SYM, Ng AM, Young JD, Herbert RB, Henderson PJ, Baldwin SA. 2004. Purification and properties of the *Escherichia coli* nucleoside transporter NupG, a paradigm for a major facilitator transporter sub-family. Mol Membr Biol 21:323–336.

59. Rosner JL, Martin RG. 2009. An excretory function for the *Escherichia coli* outer membrane pore TolC: Upregulation of *marA* and *soxS* transcription and Rob activity due to metabolites accumulated in *tolC* mutants. J Bacteriol 191:5283–5292.

60. Chubiz LM, Rao C V. 2010. Aromatic acid metabolites of *Escherichia coli* K-12 can induce the *marRAB* operon. J Bacteriol 192:4786–4789.

61. Sayed AK, Foster JW. 2009. A 750 bp sensory integration region directs global control of the *Escherichia coli* GadE acid resistance regulator. Mol Microbiol 71:1435–1450.

62. Yildiz Ö, Vinothkumar KR, Goswami P, Kühlbrandt W. 2006. Structure of the monomeric outer-membrane porin OmpG in the open and closed conformation. EMBO J 25:3702–3713.

63. de Cock H, Struyvé M, Kleerebezem M, Van Der Krift T, Tommassen J. 1997. Role of the carboxy-terminal phenylalanine in the biogenesis of outer membrane protein PhoE of *Escherichia coli* K-12. J Mol Biol 269:473–478.

64. Sardesai AA, Genevaux P, Schwager F, Ang D, Georgopoulos C. 2003. The OmpL porin does not modulate redox potential in the periplasmic space of *Escherichia coli*. EMBO J 22:1461–1466.

65. Dassa J, Fsihi H, Marck C, Dion M, Kieffer-Bontemps M, Boquet PL. 1991. A new oxygen-regulated operon in *Escherichia coli* comprises the genes for a putative third

cytochrome oxidase and for pH 2.5 acid phosphatase (*appA*). Mol Gen Genet 229:341–352.

66. Brøndsted L, Atlung T. 1996. Effect of growth conditions on expression of the acid phosphatase (*cyx-appA*) operon and the *appY* gene, which encodes a transcriptional activator of *Escherichia coli*. J Bacteriol 178:1556–1564.

67. Bertero MG, Rothery RA, Palak M, Hou C, Lim D, Blasco F, Weiner JH, Strynadka NCJ. 2003. Insights into the respiratory electron transfer pathway from the structure of nitrate reductase A. Nat Struct Biol 10:681–687.

68. Trchounian A, Sawers RG. 2014. Novel insights into the bioenergetics of mixed-acid fermentation: Can hydrogen and proton cycles combine to help maintain a proton motive force? IUBMB Life 66:1–7.

69. Sauter M, Böhm R, Böck A. 1992. Mutational analysis of the operon (*hyc*) determining hydrogenase 3 formation in *Escherichia coli*. Mol Microbiol 6:1523–1532.

70. Burstein C, Tiankova L, Kepes A. 1979. Respiratory control in *Escherichia coli* K 12. Eur J Biochem 94:387–392.

71. Rossmann R, Sawers G, Böck A. 1991. Mechanism of regulation of the formate-hydrogenlyase pathway by oxygen, nitrate, and pH: Definition of the formate regulon. Mol Microbiol 5:2807–2814.

72. McDowall JS, Murphy BJ, Haumann M, Palmer T, Armstrong FA, Sargent F. 2014. Bacterial formate hydrogenlyase complex. Proc Natl Acad Sci 111:E3948–E3956.

73. Noguchi K, Riggins DP, Eldahan KC, Kitko RD, Slonczewski JL. 2010. Hydrogenase-3 contributes to anaerobic acid resistance of *Escherichia coli*. PLoS One 5:27–29.

74. Berg BL, Li J, Heider J, Stewart V. 1991. Nitrate-inducible formate dehydrogenase in

Escherichia coli K-12. J Biol Chem 266:22380–22385.

75. Stewart V. 1993. Nitrate regulation of anaerobic respiratory gene expression in *Escherichia coli*. Mol Microbiol 9:425–434.

76. Thomason LC, Sawitzke JA, Li X, Costantino N, Court DL. 2014. Recombineering: Genetic engineering in bacteria using homologous recombination, p. 1.16.1-1.16.39. *In* Current Protocols in Molecular Biology.

77. Tschowri N, Busse S, Hengge R. 2009. The BLUF-EAL protein YcgF acts as a direct anti-repressor in a blue-light response of *Escherichia coli*. Genes Dev 23:522–534.

78. Giffard PM, Booth IR. 1988. The *rpoA341* allele of *Escherichia coli* specifically impairs the transcription of a group of positively-regulated operons. Mol Gen Genet 214:148–152.

79. Thomas MS, Glass RE. 1991. *Escherichia coli rpoA* mutation which impairs transcription of positively regulated systems. Mol Microbiol 5:2719–2725.

80. Gullberg E, Cao S, Berg OG, Ilbäck C, Sandegren L, Hughes D, Andersson DI. 2011. Selection of resistant bacteria at very low antibiotic concentrations. PLoS Pathog 7:e1002158.

81. Rath D, Jawali N. 2006. Loss of expression of *cspC*, a cold shock family gene, confers a gain of fitness in *Escherichia coli* K-12 strains. J Bacteriol 188:6780–6785.

82. Phadtare S, Inouye M. 2001. Role of CspC and CspE in regulation of expression of RpoS and UspA, the stress response proteins in *Escherichia coli* 183:1205–1214.

83. Phadtare S, Tadigotla V, Shin W, Sengupta A, Severinov K. 2006. Analysis of *Escherichia coli* global gene expression profiles in response to overexpression and deletion of CspC and CspE. J Bacteriol 188:2521–2527.

84. Cohen-Or I, Shenhar Y, Biran D, Ron EZ. 2010. CspC regulates *rpoS* transcript levels and

complements *hfq* deletions. Res Microbiol 161:694–700.

85. Sun Y, Fukamachi T, Saito H, Kobayashi H. 2012. Adenosine deamination increases the survival under acidic conditions in *Escherichia coli*. J Appl Microbiol 112:775–781.

86. McDowall JS, Murphy BJ, Haumann M, Palmer T, Armstrong FA, Sargent F. 2014. Bacterial formate hydrogenlyase complex. Proc Natl Acad Sci 111:E3948–E3956.

87. Uhlik O, Wald J, Strejcek M, Musilova L, Ridl J, Hroudova M, Vlcek C, Cardenas E, Mackova M, Macek T. 2012. Identification of bacteria utilizing biphenyl, benzoate, and naphthalene in long-term contaminated soil. PLoS One 7:e40653.

88. Davidson PM, Taylor TM, Schmidt SE. 2013. Chemical preservatives and natural antimicrobial compunds. Food Microbiol Fundam Front 4:765–801.

89. Sandberg TE, Pedersen M, LaCroix RA, Ebrahim A, Bonde M, Herrgard MJ, Palsson BO, Sommer M, Feist AM. 2014. Evolution of *Escherichia coli* to 42 °C and subsequent genetic engineering reveals adaptive mechanisms and novel mutations. Mol Biol Evol 31:2647–2662.

90. Fong SS, Joyce AR, Palsson BØ. 2005. Parallel adaptive evolution cultures of *Escherichia coli* lead to convergent growth phenotypes with different gene expression states. Genome Res 15:1365–1372.

91. Hakobyan M, Sargsyan H, Bagramyan K. 2005. Proton translocation coupled to formate oxidation in anaerobically grown fermenting *Escherichia coli*. Biophys Chem 115:55–61.

92. Lobritz MA, Belenky P, Porter CBM, Gutierrez A, Yang JH, Schwarz EG, Dwyer DJ, Khalil AS, Collins JJ. 2015. Antibiotic efficacy is linked to bacterial cellular respiration. Proc Natl Acad Sci 112:8173–8180.

93. Nishino K, Yamaguchi A. 2002. EvgA of the two-component signal transduction system

modulates production of the YhiUV multidrug transporter in *Escherichia coli*. J Bacteriol 184:2319–2323.

94. Foster JW. 2004. *Escherichia coli* acid resistance: Tales of an amateur acidophile. Nat Rev Microbiol 2:898–907.

95. Jeon YH, Yamazaki T, Otomo T, Ishihama A, Kyogoku Y. 1997. Flexible linker in the RNA polymerase alpha subunit facilitates the independent motion of the C-terminal activator contact domain. J Mol Biol 267:953–962.

96. Dangi B, Gronenborn AM, Rosner JL, Martin RG. 2004. Versatility of the carboxy-terminal domain of the α subunit of RNA polymerase in transcriptional activation: Use of the DNA contact site as a protein contact site for MarA. Mol Microbiol 54:45–59.

97. Yethon JA, Heinrichs DE, Monteiro MA, Perry MB, Whitfield C. 1998. Involvement of *waaY*, *waaQ*, and *waaP* in the modification of *Escherichia coli* lipopolysaccharide and their role in the formation of a stable outer membrane. J Biol Chem 273:26310–26316.

98. Baba T, Ara T, Hasegawa M, Takai Y, Okumura Y, Baba M, Datsenko KA, Tomita M, Wanner BL, Mori H. 2006. Construction of *Escherichia coli* K-12 in-frame, single-gene knockout mutants: The Keio collection. Mol Syst Biol 2:8.

99. Deininger KNW, Horikawa A, Kitko RD, Tatsumi R, Rosner JL, Wachi M, Slonczewski JL. 2011. A requirement of TolC and MDR efflux pumps for acid adaptation and GadAB induction in *Escherichia coli*. PLoS One 6:1–7.

100. Bhagwat AA, Ying ZI, Smith A. 2014. Evaluation of ribosomal RNA removal protocols for Salmonella RNA-Seq projects. Adv Microbiol 4:25–32.

101. Smith MW, Neidhardt FC. 1983. Proteins induced by aerobiosis in *Escherichia coli*. J Bacteriol 154:344–350.

852 **TABLES**

853 **Table 1. Strains of *Escherichia coli* used in this study[1]**

Name	Genotype	Source
W3110	*Escherichia coli* K-12	(101)
JLSK0001	W3110 benzoate-evolved A1-1	(18)
JLSK0014	W3110 benzoate-evolved C3-1	(18)
JLSK0030	W3110 benzoate-evolved G5-1	(18)
JLSK0031	W3110 benzoate-evolved G5-2	(18)
JLS0903	W3110 Δ*hyaB*::*kanR*	(73)
JLS0905	W3110 Δ*hycE*::*kanR*	(73)
JLS1010	W3110 Δ*mdtE*::*kanR*	This work
JLS1025	W3110 Δ*mdtF*::*kanR*	This work
JLS1517	W3110 Δ*gadX*::*kanR*	This work
JLS1631	W3110 Δ*cspC*::*kanR*	This work
JLS1632	W3110 Δ*gadE*::*kanR*	This work
JLS1633	W3110 Δ*rfaY*::*kanR*	This work
JLS1706	W3110 Δ*emrA*::*kanR*	(20)
JLS1732	W3110 Δ*(slp-gadX)*	This work
JLS1771	W3110 Δ*(slp-gadX)* Δ*ariR*::*kanR*	This work
JLS1777	W3110 Δ*cspC*::*kanR* Δ*rfaY*::*frt*	This work
JLS1789	W3110 Δ*add*::*kanR*	This work
JLS1820	W3110 Δ*rob*::*kanR*	This work

JLS1823	W3110 Δ*ariR*::*kanR*	This work
JLS1828	W3110 Δ*hycF*::*kanR*	This work
JLS1617	A1-1 Δ*yhdN*::*kanR rpoA*+	This work

[1]Newly isolated strains from benzoate-evolved populations (18) are listed in Supplementary Table S1.

Table 2. Mutations found in selected benzoate-evolved strains*

Generation:	900	900	1400	2000	900	900	1400	2000	900	900	1400	2000	900	900	1400	2000	2000	Mutation	Annotation	Gene
Cam:			S	S				S				S				S	S			
Strain:	A1-3	A1-4	A1-5	A1-1	A5-3	A5-4	A5-5	A5-1	C3-3	C3-4	C3-5	C3-1	G5-3	G5-4	G5-5	G5-1	G5-2			
13,291																		G→T	V377F (GTT→TTT)	*dnaK* →
56,273																		G→A	L279L (CTC→CTT)	*lptD* (*imp*)←
62,682																		+G	coding (583/2907 nt)	*hepA* ←
156,056																		T→G	N49T (AAT→ACT)	*ecpD* ←
237,555																		Δ1 bp::repeat(–) +9 bp::Δ1 bp	coding (221–229/786 nt)	*yafT* →
310,704																		(T)8→7	intergenic (–144/–632)	*ykgK* ← / → *ykgL*
490,544																		Δ6 bp	intergenic (+61/–87)	*ybaN* → / → *apt*
556,778																		A→C	F63V (TTC→GTC)	*folD* ←
573,671																		T→A	intergenic (+109/+289)	*ybcQ* → / ← *insH*
666,783																		A→T	D619E (GAT→GAA)	*mrdA* ←
683,143																		Δ5,116 bp	insH-3 IS5–mediated	[*hscC*]–*gltI*
755,210																		IS5 +8bp	intergenic (+147/–374)	*gltA* ← / *sdhC* →
907,373																		Δ1 bp	coding (1332/1431 nt)	*ybjT* ←
909,411																		G→A	P102P (CCC→CCT)	*ltaE* ←
991,031																		insH (–) +4 bp::Δ7	intergenic (–253/–10)	*pncB* ← / → *pepN*
1,213,665																		(C)8→9	intergenic (–85/+615)	*elbA* ← / ← *ycgX*
1,218,024																		IS5 (+) +4 bp	coding (79–82/267 nt)	*ariR* (*ymgB*) →
1,337,160																		G→A	intergenic (+617/–385)	*cysB* → / → *acnA*
1,349,606																		IS5 +5 bp	coding (1021/1935 nt)	*rnb* ←
1,372,264																		A→G	E112G (GAG→GGG)	*ycjM* →
1,459,205																		G→A	G354G (GGG→GGA)	*paaE* →
1,471,097																		A→G	E9G (GAA→GGA)	*insI* →
1,485,978																		C→A	R402S (CGT→AGT)	*hrpA* →
1,549,542																		IS5 (–) +4 bp	coding (428–431/3048 nt)	*fdnG* →
1,553,926																		T→C	intergenic (+221/+186)	*fdnI* → / ← *yddM*
1,574,188																		IS5 (+) +4 bp	coding (2726–2729/2796 nt)	*pqqL* ←
1,592,479																		C→A	intergenic (–229/+89)	*yneL* ← / ← *hipA*
1,618,943																		Δ6,115 bp	coding deletion	[*ydeA*]–[*ydeH*]
1,704,037																		Δ1 bp	coding (91/1002 nt)	*add* →
1,822,769																		IS5 +4 bp	coding (160/1359 nt)	*chbC* ←
1,855,048																		repeat(–) +9 bp	coding (638–646/1359 nt)	*ydjE* ←
1,881,543																		IS186/IS421 (+) +6 bp	coding (115–120/360 nt)	*yeaR* ←
1,901,989																		G→T	G437G (GGC→GGA)	*yoaE* ←
1,908,956																		Δ5::insH-4 IS5 (–) +4 bp::Δ4	coding (191–194/210 nt)	*cspC* ←
1,909,258																		IS1 (+) +9 bp	coding (40–48/144 nt)	*yobF* ←
2,093,067																		G→A	G247S (GGT→AGT)	*hisG* →
2,093,073																		G→A	E249K (GAA→AAA)	*hisG* →
2,156,723																		C→A	L191M (CTG→ATG)	*mdtA* →
2,447,095																		C→T	intergenic (–44/–115)	*fabB* ← / → *trmC*
2,646,569																		C→A	E1459* (GAG→TAG)	*yfhM* ←
2,739,952																		C→A	intergenic (–146/–64)	*aroF* ← / → *yfiL*
2,810,717																		IS2 (–) +5 bp	coding (635–639/1173 nt)	*emrA* →
2,865,825																		A→T	I89N (ATC→AAC)	*rpoS* ←
2,931,775																		C→A	P190P (CCG→CCT)	*fucA* ←
3,104,794																		G→A	G142D (GGC→GAC)	*nupG* →
3,169,126																		A→C	T215P (ACA→CCA)	*qseB* →
3,187,655																		Δ6::insH-9 IS5 (–) +4 bp::Δ5	coding (1600–1603/2466 nt)	*yqiG* →
3,188,360																		IS5 (–) +4 bp	coding (2305–2308/2466 nt)	*yqiG* →
3,189,138																		IS5 (+) +4 bp	coding (602–605/750 nt)	*yqiH* →
3,212,340																		A→C	D213A (GAC→GCC)	*rpoD* →
3,241,721																		G→T	L84M (CTG→ATG)	*uxaA* ←
3,277,113																		INDEL +5 bp	coding (257/336 nt)	*prlF* →
3,277,128																		(TTCAACA)2→3	coding (272/336 nt)	*sohA* →
3,305,846																		Δ141 bp	coding (1730–1870/1890 nt)	*deaD* ←
3,454,320																		C→T	G373S (GGC→AGC)	*rpoB* ←
3,532,025																		A→G	N107S (AAC→AGC)	*cpxA* →
3,840,032																		Δ4::insH IS5 (–) +4 bp::Δ4	coding (583–586/699 nt)	*rfaY* →
3,909,304																		Δ6::insH-11 IS5 (+) +4 bp::Δ6	intergenic (–20/–343)	*xylF* ← / → *xylA*
3,948,766																		G→A	R320H (CGT→CAT)	*bcsB* →
3,967,563																		C→A	A171S (GCG→TCG)	*yhjC* ←
3,974,646																		Δ78 bp	coding (42–119/825 nt)	*gadX* →
3,975,201																		G→T	L199F (TTG→TTT)	*gadX* →
3,975,230																		IS5 (+) +4 bp	coding (626–629/825 nt)	*gadX* →
3,976,435																		Δ10,738 bp	insH–mediated	[*gadW*]–*slp*
3,981,163																		Δ6,012 bp	repeat–mediated	[*mdtE*]–*slp*
3,986,969																		Δ204 bp	insH–mediated	*slp* ← / → *insH*
4,114,118																		C→A	intergenic (–171/–149)	*yrfF* ← / → *nudE*
4,136,677																		G→T	V191V (GTC→GTA)	*frlD*
4,200,197																		A→C	K271Q (AAA→CAA)	*rpoA* →
4,218,986																		Δ6 bp::repeat(–) +4 bp::Δ4 bp	intergenic (+187/–79)	*metA* → / → *aceB*
4,221,094																		Δ1 bp	coding (396/1305 nt)	*aceA* →
4,221,755																		G→A	A353T (GCA→ACA)	*aceA* →
4,221,855																		A→C	E386A (GAA→GCA)	*aceA* →
4,297,865																		+T	intergenic (+136/–206)	*nrfG* → / → *gltP*
4,316,928																		Δ6 bp::repeat(–) +4 bp::Δ6 bp	coding (739–742/891 nt)	*rpiR* ←
4,405,094																		G→A	V43M (GTG→ATG)	*hfq* →
4,485,284																		IS5 (–) +4 bp	coding (875–878/1197 nt)	*yjgN* →
4,543,244																		Δ4 bp::repeat(+) +4 bp::Δ6 bp	coding (199–202/1107 nt)	*yjhT* ←
4,625,980																		Δ1 bp::repeat(–) +9 bp	coding (418–426/720 nt)	*deoD* →
4,626,165																		C→G	C201W (TGC→TGG)	*deoD* →
4,639,891																		A→G	S34P (TCC→CCC)	*rob* ←

*****Highlighted generation numbers indicate published strains (18). Cam indicates chloramphenicol; S indicates loss of growth at 8µg/ml, compared to strain W3110. Colors indicate mutations in populations: A1, blue; A5, red; C3, green; G5, brown.

Table 3. Selected differentially expressed genes (Log2 fold change ≥ 1, p < 0.01) [1]

	Benzoate / No benzoate **W3110**	**A1-1 / W3110** **Benzoate**	**C3-1 / W3110** **Benzoate**	**G5-1 / W3110** **Benzoate**	**G5-2 / W3110** **Benzoate**
Up-regulated	*aceABEFK*	*acs*	*cspB*	*cvpA*	***ompF***
	appAB	*glcDE*	*pspB*	*fadB*	*ompL*
	asr	***ompF***	*phoE*	*glcDE*	*wcaADK*
	cyoABCDE		*ompG*	*ompL*	***ymgG***
	gadABC		*ompL*	*phoE*	
	gadEF			*phoH*	
	hdeB				
	hyaBF				
	hycABCDEFG				
	marRAB				
	mdtEF				
	narHJ				
	slp				
Down-regulated	*cadAB*	***appBC***	*flu*	*dctR*	*artP*
	flgBCDEFG	*dctR*	***gadABC***	***gadABC***	***asr***
	fliAFN	*flu*	***hycACDEFGH***	***gadEF***	*flu*
	fruAK	***gadABC***	*pepN*	***hdeABD***	*gltIK*
	ompF	***gadEF***	***slp***	***hycACDEFGH***	***hycCDEFG***
	ymgG	***mdtEF***		***mdtEF***	***marRB***
		hycBCDEFGH		***slp***	***slp***
		hdeABD		*sufABCD*	*yahK*
		narHIJ		*yahK*	*yeeR*
		slp		*yhiDM*	
		yeeR		*wrbA*	
		yhiDM			
		ymgG			

[1]All strains were cultured to log phase at pH 6.5, 5 mM sodium benzoate, except for the W3110 control culture without benzoate. Bold letters without underline indicate genes upregulated by benzoate in W3110 but knocked down in benzoate-evolved strains (A1-1, C3-1, G5-1, G5-2). Bold underlined indicates genes downregulated by benzoate in W3110 and that had increased expression in benzoate-evolved strains.

FIGURES

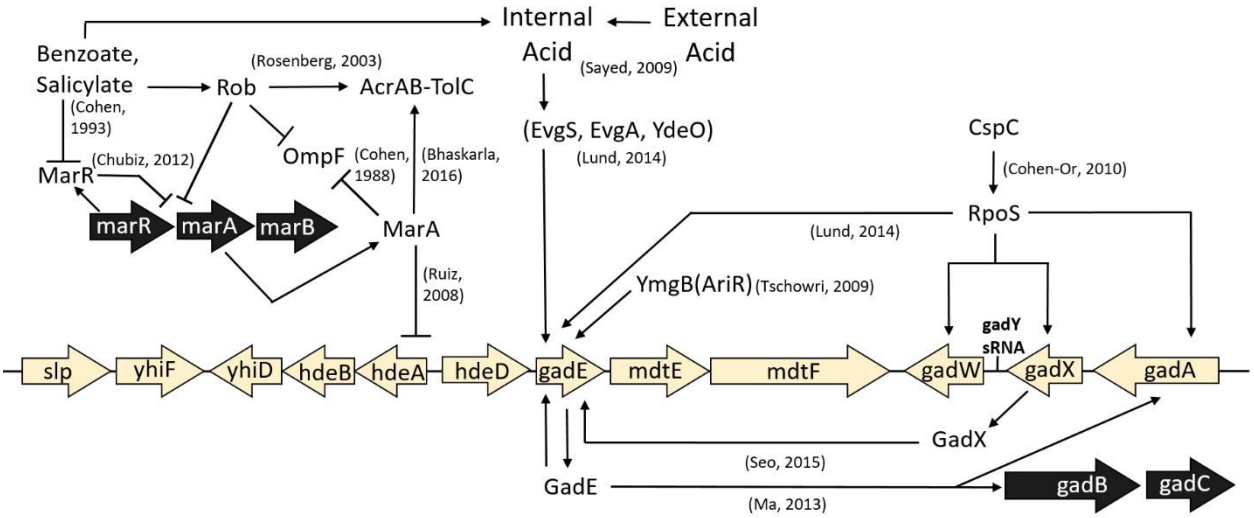

Figure 1. The Gad acid resistance regulon intersects with the Mar drug-resistance regulon. Selected components relevant to this work are shown.

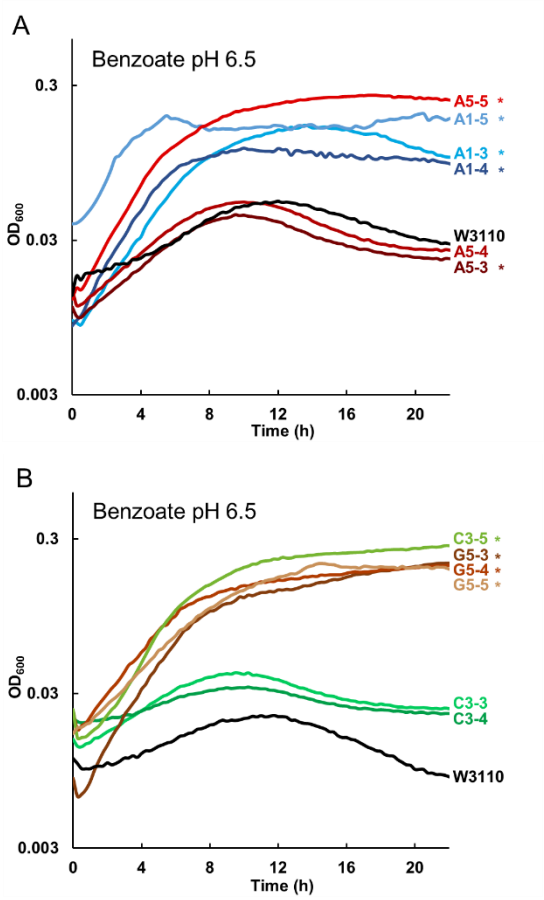

Figure 2. Isolates from early generations (500-1500 doublings) from populations A1, A5, C3, and G5. Strains were cultured in LBK 150 mM PIPES pH 6.5 with 20 mM sodium benzoate, as described under Methods. For each strain, the curve shown represents median value of OD_{600} at 16 h. Asterisk indicates significant difference from W3110, Tukey's test $p \leq 0.05$, n=4.

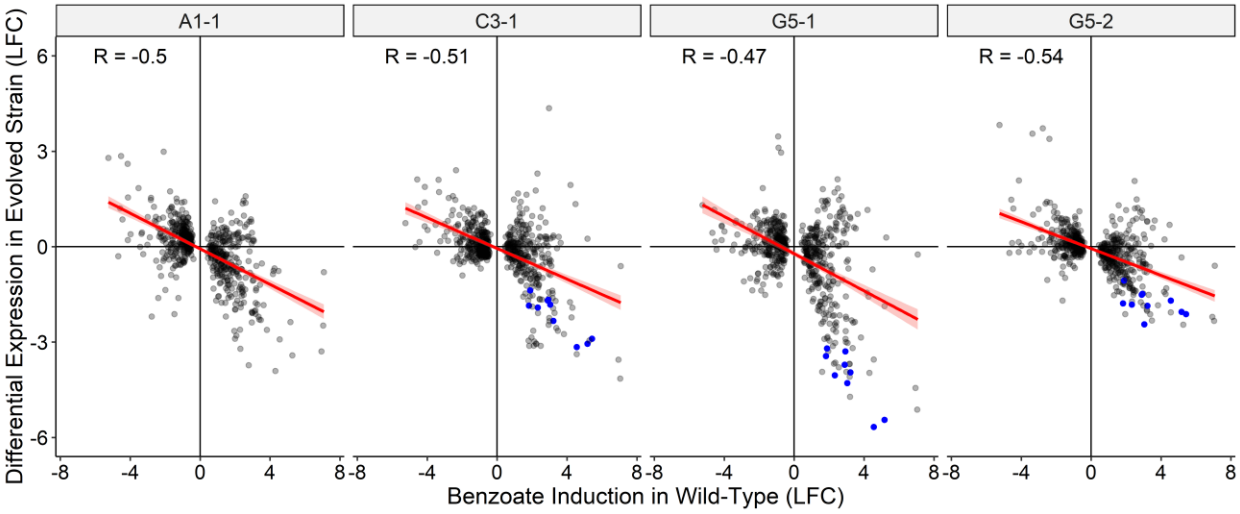

Figure 3. Genes upregulated by benzoate in the ancestral strain W3110 are downregulated in the benzoate-evolved strains. LFC=Log_2 fold change (expression ratios); data are from Supplemental File Table S3. LFC for benzoate-evolved strains over W3110 (cultured in 5 mM benzoate) are plotted as a function of LFC for W3110 with or without 5 mM benzoate. Genes shown are those significantly differentially expressed ($p < 0.001$) in at least one evolved strain. Genes of the Gad regulon (*gadAEXW*, *mdtEF*, *hdeDAB*, *slp*) and *gadBC* are colored blue. In A1-1 most of the Gad island is deleted (Δ*slp-gadW*). R is the Pearson correlation coefficient.

for each group of replicates, a curve with median OD_{600} at 16 h is presented.

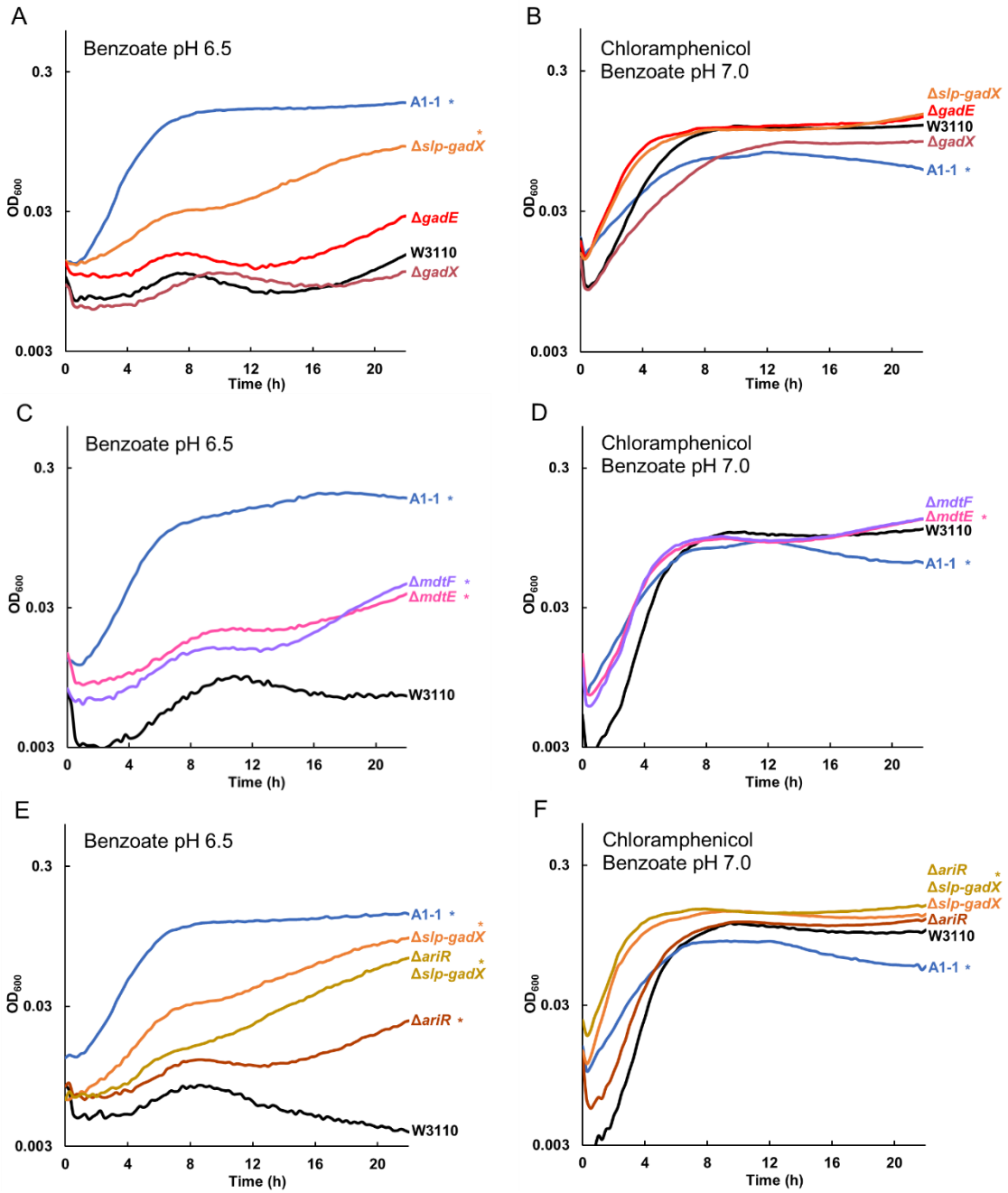

Figure 4. Gad regulon and related mutations in strain A1-1 increase growth in benzoate. Strains were cultured overnight in LBK 100 mM PIPES pH 6.5 (A, C, E) or LBK 100 mM MOPS pH 7.0 (B, D, F), both supplemented with 5 mM benzoate. Eight replicate samples from two overnight cultures (four from each) were diluted 1:200 in a 96-well plate into fresh medium; LBK 100 mM PIPES pH 6.5 supplemented with 15 mM benzoate (A, C, E) or LBK 100 mM

MOPS pH 7.0 supplemented with 5 mM benzoate and added 4 µg/ml chloramphenicol (B, D, F). For each group of replicates, a curve with median OD_{600} at 16 h is presented. Asterisk indicates significant difference from W3110 at 16 h, Tukey's test $p \leq 0.05$, n=8. **A.** W3110 constructs Δ*slp-gadX*, Δ*gadE*::*kanR*, and *ΔgadX*::*kanR* were cultured in 15 mM benzoate alongside parent strain W3110. The Δ*slp-gadX* strain grew to a higher OD_{600} than did W3110 at 16 h, though not as high as benzoate-evolved strain A1-1. **B.** Strain A1-1 and W3110 constructs Δ*slp-gadX*, Δ*gadE*::*kanR*, and Δ*gadX*::*kanR* were cultured with W3110 in benzoate and chloramphenicol. Strain A1-1 grew significantly less than W3110 at 16 h. **C.** Δ*mdtE*::*kanR* and Δ*mdtF*::*kanR* strains outgrew W3110 in benzoate, but did not grow as high as A1-1. **D.** Δ*mdtE*::*kanR* and Δ*mdtF*::*kanR* strains grew higher than W3110 in 5 mM benzoate with chloramphenicol, whereas strain A1-1 reached a lower OD_{600} at 16 h. **E.** Δ*ariR*::*kanR* had increased growth in benzoate, but not as high as Δ*slp-gadX*, Δ*ariR*::*kanR* Δ*slp-gadX*, or A1-1. **F.** While Δ*ariR*::*kanR* and Δ*slp-gadX* did not affect growth in benzoate with chloramphenicol, Δ*ariR*::*kanR* Δ*slp-gadX* outgrew the ancestor W3110.

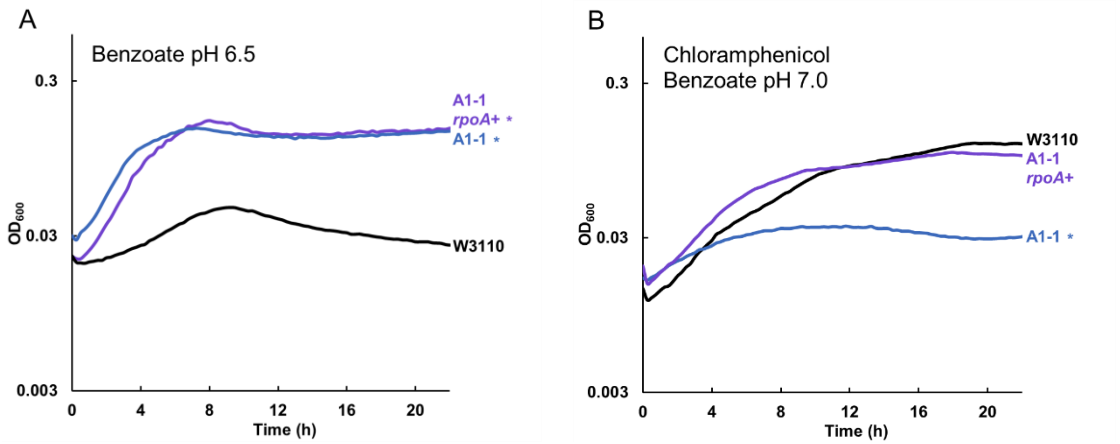

Figure 5. Chloramphenicol sensitivity with *rpoA* K271Q replacement by *rpoA*$^+$ in A1-1. **A.** Construct A1-1 with *rpoA* K271Q reversion to *rpoA*$^+$ (A1-1 Δ*yhdN*::*kanR rpoA*$^+$) showed no significant difference from A1-1 (cultured with 15 mM benzoate). **B.** A1-1 Δ*yhdN*::*kanR rpoA*$^+$ grew to a comparable level as W3110 in 8 µg/ml chloramphenicol with 5 mM benzoate. Culture conditions for panels A, B were the same as for Figure 4 A, B respectively, except that the chloramphenicol concentration was 8 µg/ml (B).

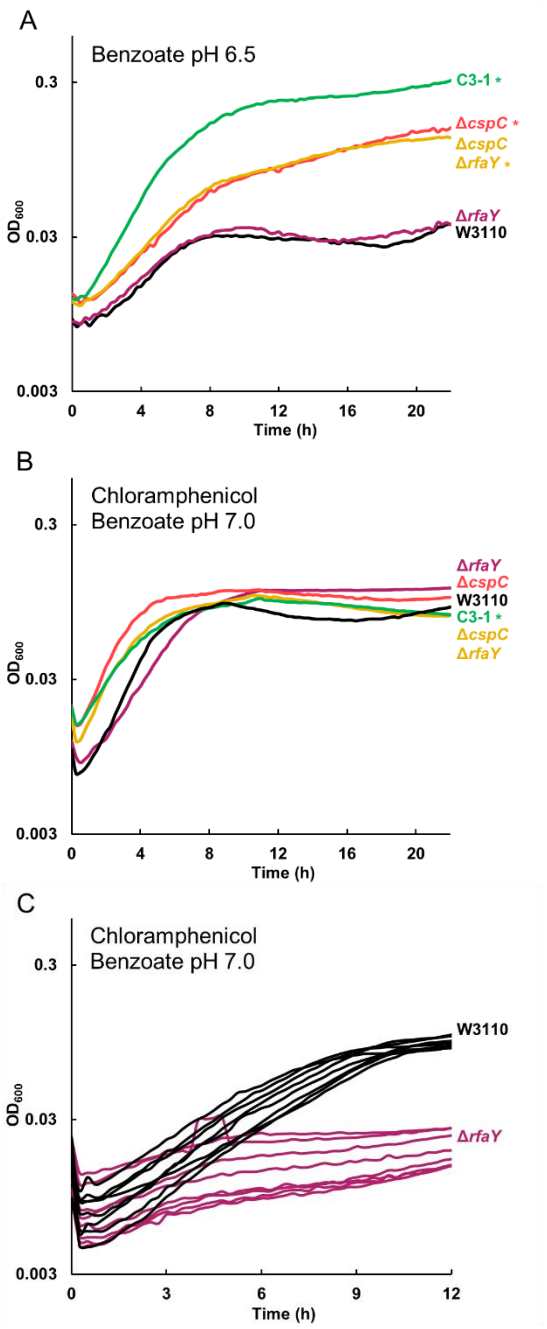

Figure 6. *cspC* deletion confers benzoate tolerance and deletion of *rfaY* confers chloramphenicol sensitivity. **A.** In 15 mM benzoate, W3110 Δ*cspC* reached higher growth than W3110, but W3110 Δ*rfaY* showed no growth difference from W3110. The Δ*cspC* Δ*rfaY* growth curve resembled that of Δ*cspC*. **B.** W3110 constructs Δ*rfaY*::*kanR* and Δ*cspC*::*kanR* Δ*rfaY*::*frt* showed no difference from W3110 at 16 h, but Δ*rfaY*::*kanR* had a lower log-phase growth-rate compared

to W3110 in 5 mM benzoate with 4 µg/ml chloramphenicol. **C.** At 8 µg/ml chloramphenicol, 5 mM benzoate, W3110 Δ*rfaY*::*kanR* has lower log-phase growth rate than W3110 (t-test $p < 0.01$); for each strain, 8 individual replicates are shown.

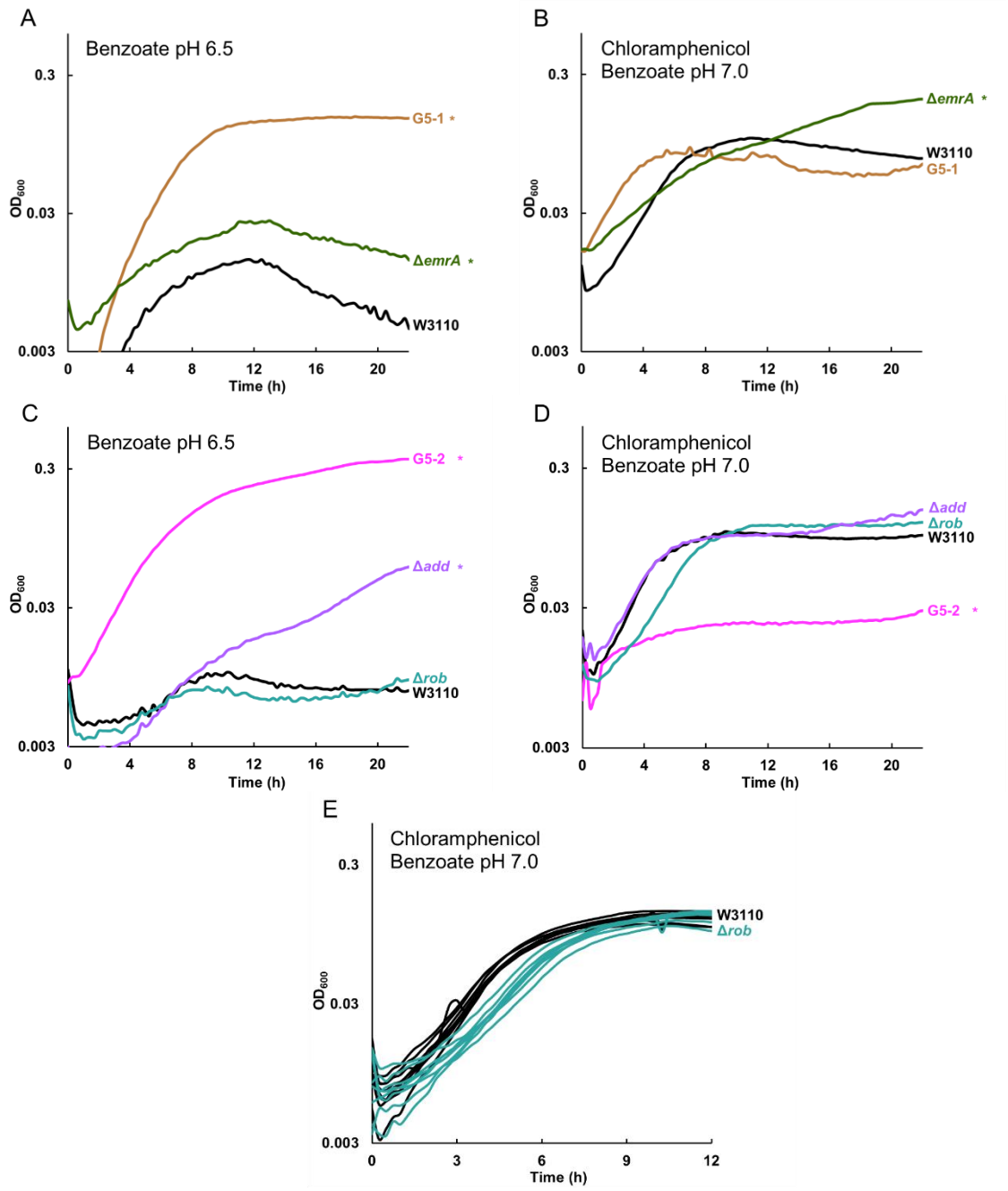

Figure 7. Δ*add* confers benzoate tolerance, and Δ*rob* decreases log-phase growth rate in chloramphenicol **A.** Strains G5-1 and W3110 Δ*emrA*::*kanR* outgrew W3110 at 16 h, in 15 mM benzoate. **B.** W3110 Δ*emrA* outgrew W3110 and G5-1 at 16 h, in 5 mM benzoate, 4 µg/ml chloramphenicol. **C.** G5-2 and W3110 Δ*add*::*kanR* outgrew W3110 in 15 mM benzoate. Δ*rob*::*kanR* did not affect growth. **D.** W3110 Δ*add*::*kanR*, W3110 Δ*rob*::*kanR*, and W3110

showed no difference in 5 mM benzoate, 4 µg/ml chloramphenicol. Strain G5-2 grew less than W3110. **E.** Δ*rob*::*kanR* conferred a lower log-phase growth rate in 5 mM benzoate, 4 µg/ml chloramphenicol (t-test $p < 0.01$). 8 replicates per strain are shown.

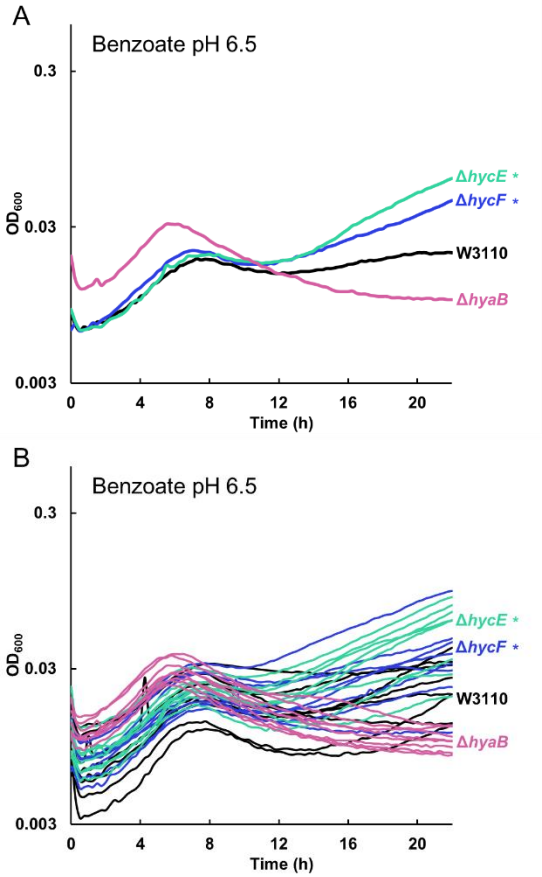

Figure 8. Deletion of hydrogenase Hyd-3 enhances late growth in 15 mM benzoate pH 6.5. W3110 with Δ*hycE*::*kanR* or Δ*hycF*::*kanR* grows to higher median value of OD_{600} at 20 h than that of the parent W3110. The W3110 Δ*hyaB*::*kanR* strain deleted for Hyd-1 shows no enhancement of late growth compared to W3110. **A.** Median growth curves presented for each set of 8 replicates. **B.** All 8 replicates shown for each strain.